# Carborane Complexes of Ruthenium: Reactions of [Ru(THF)(CO)$_2$($\eta^5$-7,8-R$_2$-7,8-C$_2$B$_9$H$_9$)] (R = H or Me) with Alkylidyne Complexes of Molybdenum and Tungsten†

Stephen Anderson,‡ John C. Jeffery,§ Yi-Hsien Liao,‡ Donald F. Mullica,‡ Eric L. Sappenfield,‡ and F. Gordon A. Stone*,‡

*Department of Chemistry, Baylor University, Waco, Texas 76798-7348, and School of Chemistry, University of Bristol, Bristol BS8 1TS, U.K.*

*Received November 1, 1996*⊗

The complex [Ru(THF)(CO)$_2$($\eta^5$-7,8-C$_2$B$_9$H$_{11}$)] (**1a**, THF = tetrahydrofuran) reacts with the alkylidyne reagents [M(≡CC$_6$H$_4$Me-4)(CO)$_2$($\eta^5$-C$_5$H$_5$)] (M = Mo or W) to give the compounds [MRu($\mu$-CC$_6$H$_4$Me-4)(CO)$_4$($\eta^5$-7,8-C$_2$B$_9$H$_{11}$)($\eta^5$-C$_5$H$_5$)] (M = W (**2a**), Mo (**2b**)), which readily isomerize to the species [MRu(CO)$_4${$\sigma$,$\eta^5$-9-CH(C$_6$H$_4$Me-4)-7,8-C$_2$B$_9$H$_{10}$}($\eta^5$-C$_5$H$_5$)] (M = W (**3a**), Mo (**3b**)). The structure of **3b** was established by X-ray diffraction. The Mo(CO)$_2$($\eta^5$-C$_5$H$_5$) fragment is attached to the *closo*-RuC$_2$B$_9$ framework by a Mo−Ru bond and a three-center two-electron B−H⇀Mo linkage involving a boron atom in an α site in the CC*B*BB ring ligating the ruthenium. The CH(C$_6$H$_4$Me-4) moiety bridges between the Ru(CO)$_2$ group and the B atom located in the other α site in the CCBB*B* ring. The oxo complex [WRuO{$\mu$-$\sigma$,$\eta^5$-9-CH(C$_6$H$_4$Me-4)-7,8-C$_2$B$_9$H$_{10}$}(CO)$_2$($\eta^5$-C$_5$H$_5$)] (**4a**) is a side product in the formation of **3a**, and it also was characterized by X-ray diffraction. Treatment of the species **3** with PMe$_3$ affords the zwitterionic compounds [MRu(CO)$_4${$\eta^5$-9-CH(PMe$_3$)(C$_6$H$_4$Me-4)-7,8-C$_2$B$_9$H$_{10}$}($\eta^5$-C$_5$H$_5$)] (M = W (**5a**), Mo (**5b**)). A single-crystal X-ray diffraction study of **5a** revealed that the (OC)$_2$W−Ru(CO)$_2$ unit is bridged by the *nido*-9-CH(PMe$_3$)(C$_6$H$_4$Me-4)-7,8-C$_2$B$_9$H$_{10}$ group. The open C$_2$B$_3$ face is pentacoordinated to the Ru atom, and there is an exopolyhedral B−H⇀W bond involving a B$_\alpha$ atom in the CC*B*BB ring. The other B$_\alpha$ site carries the CH(PMe$_3$)(C$_6$H$_4$Me-4) substituent. Reactions between the ruthenium reagent [Ru(THF)(CO)$_2$($\eta^5$-7,8-Me$_2$-7,8-C$_2$B$_9$H$_9$)] (**1b**) and [W(≡CC$_6$H$_4$Me-4)(CO)$_2$($\eta^5$-C$_5$H$_5$)] gave [WRuO{$\mu$-$\sigma$,$\eta^5$-7,8-Me$_2$-10-CH(C$_6$H$_4$Me-4)-7,8-C$_2$B$_9$H$_8$}(CO)$_2$($\eta^5$-C$_5$H$_5$)] (**4b**), [WRu($\mu$-H){$\mu$-$\eta^5$,$\eta'^5$-7,8-Me$_2$-9-C$_5$H$_4$-10-CH$_2$(C$_6$H$_4$Me-4)-7,8-C$_2$B$_9$H$_7$}(CO)$_5$] (**6a**), and [WRu{$\mu$-$\sigma$,$\eta^5$-2,7-Me$_2$-8-CH$_2$(C$_6$H$_4$-Me-4)-9-C(H)O-2,7-C$_2$B$_9$H$_6$}(CO)$_4$($\eta^5$-C$_5$H$_5$)] (**7a**) that were separated by column chromatography. The corresponding reaction between **1b** and [W(≡CC$_6$H$_4$Me-2)(CO)$_2$($\eta^5$-C$_5$H$_5$)] afforded [WRuO-{$\mu$-$\sigma$,$\eta^5$-7,8-Me$_2$-*n*-CH(C$_6$H$_4$Me-2)-7,8-C$_2$B$_9$H$_8$}(CO)$_2$($\eta^5$-C$_5$H$_5$)] (*n* = 9 (**4c**), 10 (**4d**)) and [WRu{$\mu$-$\sigma$,$\eta^5$-2,7-Me$_2$-8-CH$_2$(C$_6$H$_4$Me-2)-9-C(H)O-2,7-C$_2$B$_9$H$_6$}(CO)$_4$($\eta^5$-C$_5$H$_5$)] (**7b**). Treatment of **1b** with [Mo(≡CC$_6$H$_4$Me-*n*)(CO)$_2$($\eta^5$-C$_5$H$_5$)] (*n* = 4 or 2) yielded [MoRu($\mu$-H){$\mu$-$\eta^5$,$\eta'^5$-7,8-Me$_2$-9-C$_5$H$_4$-10-CH$_2$(C$_6$H$_4$Me-*n*)-7,8-C$_2$B$_9$H$_7$}(CO)$_5$] (*n* = 4 (**6b**), 2 (**6c**)). The structures of **4b**, **6b**, and **7b** were established by X-ray diffraction. In **6b**, the (OC)$_3$Mo($\mu$-H)Ru(CO)$_2$ unit is bridged by a 7,8-Me$_2$-9-C$_5$H$_4$-10-CH$_2$(C$_6$H$_4$Me-4)-7,8-C$_2$B$_9$H$_7$ moiety, a structure resulting from a linking of C$_5$H$_5$ and *nido*-C$_2$B$_9$ groups. The C$_5$ ring is $\eta^5$-coordinated to the molybdenum, while the open CCBBB face of the carborane cage is similarly attached to the ruthenium. In complex **7b**, a *nido*-2,7-Me$_2$-8-CH$_2$(C$_6$H$_4$Me-2)-9-C(H)O-2,7-C$_2$B$_9$H$_6$ cage system bridges the Ru−W bond with an $\eta^5$-CB$_4$ ring coordinated to the Ru atom and with the cage joined to the W atom by a B−W bond. In addition, the C(H)O group forms a second bridge linking the cage to the tungsten, with the latter coordinated by the formyl O atom.



## Introduction

The ruthenium complexes [Ru(CO)$_3$($\eta^5$-7,8-R$_2$-7,8-C$_2$B$_9$H$_9$)] (R = H or Me) are interesting metallacarboranes on account of their isolobal relationship with the well-known cyclopentadienyl species [M(CO)$_3$($\eta^5$-C$_5$R′$_5$)] (M = Mn or Re, R′ = H or Me). The latter are important precursors to many organo-manganese and -rhenium compounds; hence, it is likely that the ruthenium species will also display an extensive chemistry. Although the compound [Ru(CO)$_3$($\eta^5$-7,8-C$_2$B$_9$H$_{11}$)] has been known for some years,[1,2] it has only become readily available through a new synthesis, thus, allowing its chemistry to be explored.[3a] The related complex [Ru(CO)$_3$($\eta^5$-7,8-Me$_2$-7,8-C$_2$B$_9$H$_9$)] has been obtained recently.[3b] Both ruthenium compounds on treatment with [NEt$_4$]I afford iodo complexes [NEt$_4$][RuI(CO)$_2$($\eta^5$-7,8-R$_2$-7,8-C$_2$B$_9$H$_9$)], and these in turn react with AgBF$_4$

* To whom correspondence should be addressed.

† In the compounds described in this paper, ruthenium atoms and *nido*-C$_2$B$_9$ cages form *closo*-1,2-dicarba-3-ruthenadodecaborane frameworks which have exopolyhedral bonds to other metal centers. In order to avoid a complex nomenclature and cage numbering system for the dimetal species, following precedent (Mullica, D. F.; Sappenfield, E. L.; Stone, F. G. A.; Woollam, S. F. *Organometallics* **1994**, *13*, 157), we treat the C$_2$B$_9$ fragments as *nido*-11-vertex ligands and number as for an icosahedron from which the twelfth vertex has been removed. This has the added convenience of relating the metallacarborane complexes to isolobal species with $\eta^5$-C$_5$H$_5$ ligands.

‡ Baylor University.

§ University of Bristol.

⊗ Abstract published in *Advance ACS Abstracts,* February 1, 1997.

(1) Siedle, A. R. *J. Organomet. Chem.* **1975**, *90*, 249.
(2) Behnken, P. E.; Hawthorne, M. F. *Inorg. Chem.* **1984**, *23*, 3420.

S0276-7333(96)00928-4 CCC: $14.00 

in THF (tetrahydrofuran) to yield the reagents [Ru(THF)$(CO)_2(\eta^5$-7,8-$R_2$-7,8-$C_2B_9H_9)$] (R = H (**1a**), Me (**1b**)), which function as useful sources of $Ru(CO)_2(\eta^5$-7,8-$R_2$-7,8-$C_2B_9H_9)$ groups in synthesis.[3c,d] The methodology is in principal related to the generation of the labile species $[Mn(THF)(CO)_2(\eta^5\text{-}C_5H_5)]$ from $[Mn(CO)_3(\eta^5\text{-}C_5H_5)]$.

Extensive studies have shown that the ligating properties of alkynes are mimicked by the alkylidyne complexes $[M(\equiv CR')(CO)_2(\eta^5\text{-}C_5H_5)]$ (M = Mo or W, R′ = alkyl, aryl, or alkynyl). On the basis of this isolobal mapping,[4] numerous compounds with heteronuclear metal−metal bonds have been synthesized by treating the alkylidyne complexes with coordinatively unsaturated metal−ligand fragments.[5] Applications of the methodology to metallacarborane chemistry[6] include the preparation of $[MoW(\mu\text{-}CC_6H_4Me\text{-}4)(CO)_3(\eta^5\text{-}7,8\text{-}Me_2\text{-}7,8\text{-}C_2B_9H_9)(\eta^5\text{-}C_5H_5)]$ by addition of $[W(\equiv CC_6H_4Me\text{-}4)(CO)_2(\eta^5\text{-}C_5H_5)]$ to the coordinatively unsaturated fragment $Mo(CO)_2(\eta^5\text{-}7,8\text{-}Me_2\text{-}7,8\text{-}C_2B_9H_9)$, generated by protonation of $[NEt_4][Mo(CO)_2(\eta^5\text{-}7,8\text{-}Me_2\text{-}7,8\text{-}C_2B_9H_9)(\eta^3\text{-}C_3H_5)]$,[7a] and treatment of $[Mo(CO)_4(\eta^5\text{-}7,8\text{-}Me_2\text{-}10\text{-}OEt\text{-}7,8\text{-}C_2B_9H_8)]$ with $[W(\equiv CC_6H_4Me\text{-}4)(CO)_2(\eta^5\text{-}C_5H_5)]$ to yield $[MoW(\mu\text{-}CC_6H_4Me\text{-}4)(CO)_3(\eta^5\text{-}7,8\text{-}Me_2\text{-}10\text{-}OEt\text{-}7,8\text{-}C_2B_9H_8)(\eta^5\text{-}C_5H_5)]$.[7b] The observation that the reagent **1a** with PhC≡CPh affords the alkyne complex $[Ru(CO)_2(PhC{\equiv}CPh)(\eta^5\text{-}7,8\text{-}C_2B_9H_{11})]$[3c] suggested that both labile THF adducts **1** would similarly react with the alkylidyne complexes $[M(\equiv CR')(CO)_2(\eta^5\text{-}C_5H_5)]$ to afford new dimetal compounds of formulation $[MRu(\mu\text{-}CR')(CO)_4(\eta^5\text{-}7,8\text{-}R_2\text{-}7,8\text{-}C_2B_9H_9)(\eta^5\text{-}C_5H_5)]$, Chart 1. Such products with their unsaturated dimetallacyclopropene groups M(μ-CR′)Ru would be expected to be reactive precursors to cluster compounds.[5] In practice, although such dimetal complexes are formed initially, they undergo further reaction to give a complex mixture of heteronuclear dimetal products which are described herein.

## Results and Discussion

The complex **1a**, generated from $[NEt_4][RuI(CO)_2(\eta^5\text{-}7,8\text{-}C_2B_9H_{11})]$ and $AgBF_4$ in THF and used *in situ*, reacts with $[W(\equiv CC_6H_4Me\text{-}4)(CO)_2(\eta^5\text{-}C_5H_5)]$ in $CH_2Cl_2$ to give the red crystalline dimetal complex $[WRu(\mu\text{-}CC_6H_4Me\text{-}4)(CO)_4(\eta^5\text{-}7,8\text{-}C_2B_9H_{11})(\eta^5\text{-}C_5H_5)]$ (**2a**), characterized by the data given in Tables 1 and 2. In the $^1H$ NMR spectrum, a diagnostic resonance for the cage CH protons is seen at δ 2.00, while in the $^{13}C\{^1H\}$ spectrum, a peak for the cage carbon atoms occurs at δ 41.9.[6b] Typically, in the spectra of dimetal complexes with bridging tolylmethylidyne groups, the signals for the $\mu\text{-}CC_6H_4Me\text{-}4$ nuclei are in the range δ 325−425.[8] For example, in the $^{13}C\{^1H\}$ NMR spectrum of the aforementioned compound $[MoW(\mu\text{-}CC_6H_4Me\text{-}4)(CO)_3(\eta^5\text{-}7,8\text{-}Me_2\text{-}7,8\text{-}C_2B_9H_9)(\eta^5\text{-}C_5H_5)]$, the signal is at δ 380.1.[7a] In the spectrum of **2a**, the peak seen at δ 301.9 must be assigned to the μ-C nucleus, a value differing little from that for the terminal alkylidyne carbon (δ 300.0) in the precursor $[W(\equiv CC_6H_4Me\text{-}4)(CO)_2(\eta^5\text{-}C_5H_5)]$. Several X-ray diffraction studies have shown that in situations where a $\mu\text{-}CC_6H_4Me\text{-}4$ moiety in a dimetal species asymmetrically bridges a metal−metal bond, with the result that the C≡W bond is little perturbed, the $^{13}C$ NMR shift for the $\mu\text{-}CC_6H_4Me\text{-}4$ nucleus is at ca. 300 ppm.[9] We conclude that such asymmetric bridging by the alkylidyne ligand seems likely in **2a**.

It is evident that the CO groups in the molecule undergo site exchange under the conditions of measurement because only one broad CO resonance for these ligands is observed in the $^{13}C\{^1H\}$ NMR spectrum at room temperature and the chemical shift lies intermediate between that for RuCO and WCO groups. A somewhat unusual feature of the $^1H$ NMR spectrum is the observation of a singlet for the aryl protons. In complexes with $CC_6H_4Me\text{-}4$ groups, these customarily appear either as an unresolved multiplet or with an $(AB)_2$ pattern, as occurs in the spectra of several complexes listed in Table 2. However, the observation of a singlet has precedent.[10]

By analogy with the previous synthesis of the alkyne complex $[Ru(CO)_2(PhC{\equiv}CPh)(\eta^5\text{-}7,8\text{-}C_2B_9H_{11})]$,[3c] formation and isolation of **2a** was anticipated. However, species predicted by isolobal mapping are not necessarily thermodynamically stable.[4a] This is so with **2a** which, after stirring for several hours in $CH_2Cl_2$, isomerizes to form $[WRu(CO)_4\{\sigma,\eta^5\text{-}9\text{-}CH(C_6H_4Me\text{-}4)\text{-}7,8\text{-}C_2B_9H_{10}\}(\eta^5\text{-}C_5H_5)]$ (**3a**). The reaction between **1a** and $[Mo(\equiv CC_6H_4Me\text{-}4)(CO)_2(\eta^5\text{-}C_5H_5)]$ initially affords $[MoRu(\mu\text{-}CC_6H_4Me\text{-}4)(CO)_4(\eta^5\text{-}7,8\text{-}C_2B_9H_{11})(\eta^5\text{-}C_5H_5)]$ (**2b**), but the latter is much more labile than its tungsten analog **2a** and readily rearranges into $[MoRu(CO)_4\{\sigma,\eta^5\text{-}9\text{-}CH(C_6H_4Me\text{-}4)\text{-}7,8\text{-}C_2B_9H_{10}\}(\eta^5\text{-}C_5H_5)]$ (**3b**). The lability of **2b** prevented the acquisition of reliable microanalytical or $^{13}C\{^1H\}$ NMR data, but it was possible to measure the $^1H$ and $^{11}B\{^1H\}$ NMR spectra (Table 2), which closely resembled those of **2a**. Thus, there is little doubt that **2b** lies on the pathway to **3b**.

Repeated attempts to grow crystals of **3a** for an X-ray diffraction study were unsuccessful. Fortunately, it was possible to obtain a suitable crystal of the molybdenum analog **3b**. The molecule is shown in Figure 1, and selected data are listed in Table 3. The $Mo(CO)_2(\eta^5\text{-}C_5H_5)$ fragment is attached to the icosahedral $RuC_2B_9$ framework by a Mo−Ru bond (2.976(1) Å) and by a

(3) (a) Anderson, S.; Mullica, D. F.; Sappenfield, E. L.; Stone, F. G. A. *Organometallics* **1995**, *14*, 3516. (b) Liao, Y-H.; Mullica, D. F.; Sappenfield, E. L.; Stone, F. G. A. *Organometallics* **1996**, *15*, 5102. (c) Anderson, S.; Mullica, D. F.; Sappenfield, E. L.; Stone, F. G. A. *Organometallics* **1996**, *15*, 1676. (d) Jeffery, J. C.; Jellis, P. A.; Liao, Y-H.; Stone, F. G. A. unpublished results.

(4) (a) Hoffmann, R. *Angew. Chem., Int. Ed. Engl.* **1982**, *21*, 711. (b) Stone, F. G. A. *Angew. Chem., Int. Ed. Engl.* **1984**, *23*, 89.

(5) Stone, F. G. A. *Pure Appl. Chem.* **1986**, *58*, 529. Stone, F. G. A. in *Advances in Metal Carbene Chemistry*; Kluwer Academic Publishers: Dordrecht, The Netherlands, 1989. Davies, S. J.; Howard, J. A. K.; Musgrove, R. J.; Stone, F. G. A. *J. Chem. Soc., Dalton Trans.* **1989**, 2269 and references cited therein.

(6) (a) Stone, F. G. A. *Adv. Organomet. Chem.* **1990**, *31*, 53. (b) Brew, S. A.; Stone, F. G. A. *Adv. Organomet. Chem.* **1993**, *35*, 135. (c) Jelliss, P. A.; Stone, F. G. A. *J. Organomet. Chem.* **1995**, *500*, 307.

(7) (a) Dossett, S. J.; Li, S.; Stone, F. G. A. *J. Chem. Soc., Dalton Trans.* **1993**, 1585. (b) Mullica, D. F.; Sappenfield, E. L.; Stone, F. G. A.; Woollam, S. F. *Organometallics* **1994**, *13*, 157.

(8) Dossett, S. J.; Hill, A. F.; Jeffery, J. C.; Marken, F.; Sherwood, P.; Stone, F. G. A. *J. Chem. Soc., Dalton Trans.* **1988**, 2453.

(9) (a) Devore, D. D.; Howard, J. A. K; Jeffery, J. C.; Pilotti, M. U.; Stone, F. G. A. *J. Chem. Soc., Dalton Trans.* **1989**, 303. (b) Carr, N.; Gimeno, M. C.; Goldberg, J. E.; Pilotti, M. U.; Stone, F. G. A.; Topaloğlu, I. *J. Chem. Soc., Dalton Trans.* **1990**, 2253. (c) Carr, N.; Gimeno, M. C.; Stone, F. G. A. *J. Chem. Soc., Dalton Trans.* **1990**, 2617. (d) Jeffery, J. C.; Mortimer, M. D.; Stone, F. G. A. *Inorg. Chim. Acta* **1992**, *198*, 593.

(10) Carriedo, G. A.; Howard, J. A. K.; Stone, F. G. A. *J. Chem. Soc., Dalton Trans.* **1984**, 1555. Jeffery, J. C.; Parrott, M. J.; Pyell, U.; Stone, F. G. A. *J. Chem. Soc., Dalton Trans.* **1988**, 1121. Hart, I. J.; Jeffery, J. C.; Grosse-Ophoff, M. J.; Stone, F. G. A. *J. Chem. Soc., Dalton Trans.* **1988**, 1867.

**Chart 1**

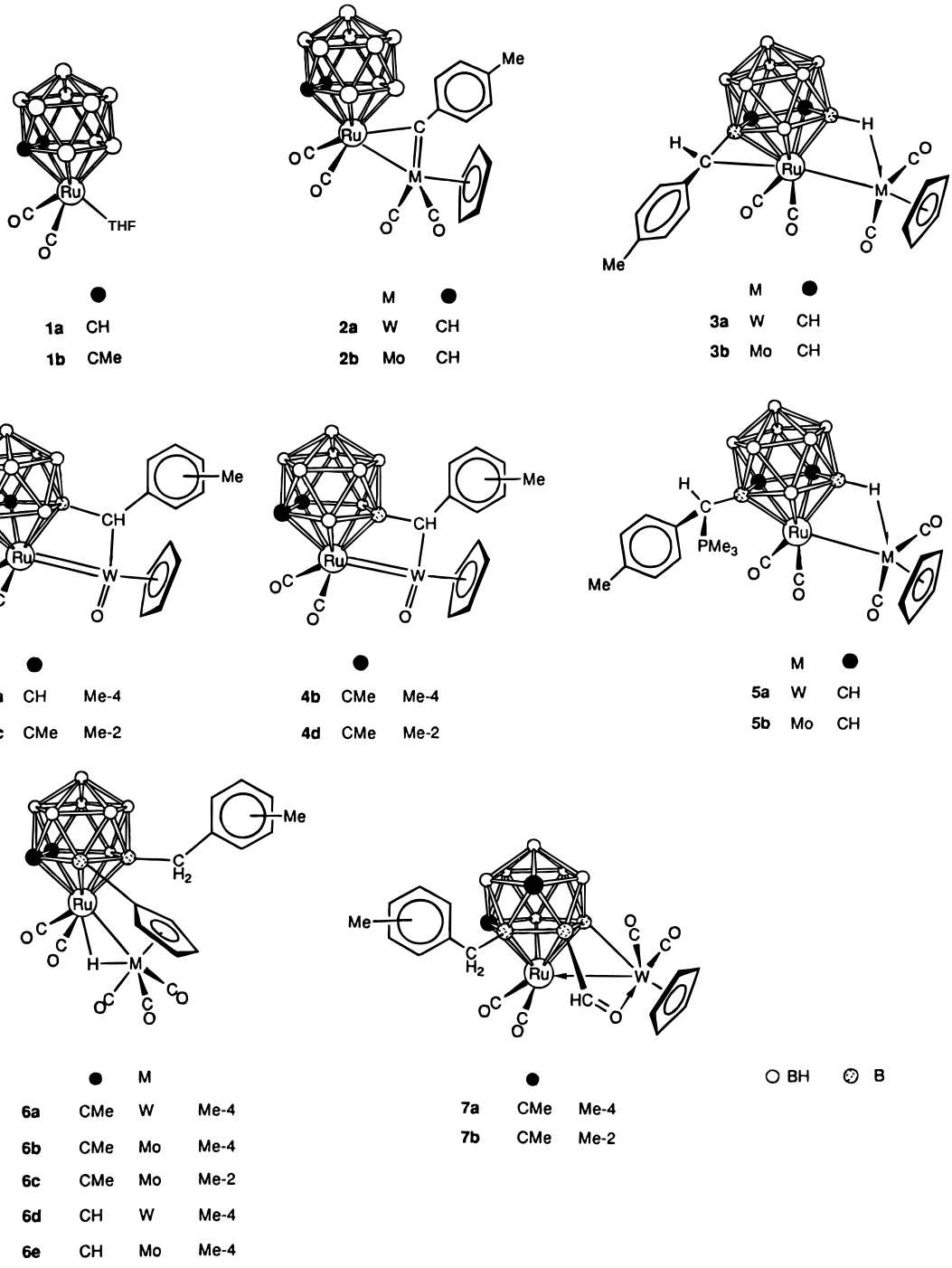


| | | |
|---|---|---|
| **1a** | CH | |
| **1b** | CMe | |

| | | | |
|---|---|---|---|
| **2a** | W | CH | |
| **2b** | Mo | CH | |

| | | | |
|---|---|---|---|
| **3a** | W | CH | |
| **3b** | Mo | CH | |

| | | | |
|---|---|---|---|
| **4a** | CH | | Me-4 |
| **4c** | CMe | | Me-2 |

| | | | |
|---|---|---|---|
| **4b** | CMe | | Me-4 |
| **4d** | CMe | | Me-2 |

| | | | |
|---|---|---|---|
| **5a** | W | CH | |
| **5b** | Mo | CH | |

| | | | |
|---|---|---|---|
| **6a** | CMe | W | Me-4 |
| **6b** | CMe | Mo | Me-4 |
| **6c** | CMe | Mo | Me-2 |
| **6d** | CH | W | Me-4 |
| **6e** | CH | Mo | Me-4 |

| | | |
|---|---|---|
| **7a** | CMe | Me-4 |
| **7b** | CMe | Me-2 |



three-center two-electron B−H→Mo linkage with B(5) (Mo−B(5) = 2.486(5) Å, Mo−H(5) = 1.83 Å, B(5)−H(5) = 1.15 Å). Each metal atom is coordinated by two CO molecules, but with some deviation (ca. 6°) from linearity in the Mo(or Ru)−C−O linkages (Table 3). Interest centers on the C(H)$C_6H_4$Me-4 moiety which bridges the B(3)−Ru connectivity (B(3)−C(10) = 1.512(6) Å, B(3)−Ru = 2.166(4) Å, C(10)−Ru 2.351(4) Å). This structural feature, in which the CH($C_6H_4$Me-4) group is exopolyhedrally bound to the *nido*-7,8-$C_2B_9$ framework while also forming a $\sigma$ bond to the metal atom, which is pentacoordinated by the open $C_2B_3$ face of the cage, has been found previously in the molecules [$NEt_4$][$Mo(CO)_3$-{$\sigma,\eta^5$-7,8-$Me_2$-10-CH($C_6H_4$Me-4)-7,8-$C_2B_9H_8$}],[11] [Rh(CO)($PPh_3$){$\sigma,\eta^5$-7,8-$R_2$-10-CH($C_6H_4$Me-4)-7,8-$C_2B_9H_8$}] (R = H,[12a] Me[12b]), and [MoW($\mu$-$C_4Me_4$){$\sigma,\eta^5$-7,8-$Me_2$-10-CH($C_6H_4$Me-4)-7,8-$C_2B_9H_8$}($\eta^5$-$C_7H_7$)],[13] although in these four structures the CH($C_6H_4$Me-4) group is attached to the boron atom in the $\beta$ site in the $\overline{\text{CCB}B\text{B}}$ ring rather than to an α site $\overline{\text{CC}B\text{BB}}$ as in **3b**. In the latter compound, the CH($C_6H_4$Me-4) moiety evidently results from insertion of the $\mu$-tolylmethylidyne unit in **2b** into a $B_\alpha$−H bond in the cage. The remaining $B_\alpha$

(11) Devore, D. D.; Emmerich, C.; Howard, J. A. K.; Stone, F. G. A. *J. Chem. Soc., Dalton Trans.* **1989**, 797.
(12) (a) Pilotti, M. U.; Stone, F. G. A. *J. Chem. Soc., Dalton Trans.* **1990**, 2625. (b) Pilotti, M. U.; Stone, F. G. A.; Topaloğlu, I. *J. Chem. Soc., Dalton Trans.* **1991**, 1621.
(13) Dossett, S. J.; Hart, I. J.; Pilotti, M. U.; Stone, F. G. A. *J. Chem. Soc., Dalton Trans.* **1991**, 511.

**Table 1. Physical and Infrared Absorption Data**

| compd | color | yield/ % | $\nu_{max}$(CO)[a]/cm$^{-1}$ | anal./%[b] C | H |
|---|---|---|---|---|---|
| [WRu($\mu$-CC$_6$H$_4$Me-4)(CO)$_4$($\eta^5$-7,8-C$_2$B$_9$H$_{11}$)($\eta^5$-C$_5$H$_5$)] (**2a**) | red | 49 | 2045 s, 2013 m, 1981 m, 1965 sh | 32.2 (32.7) | 3.4 (3.3) |
| [MoRu($\mu$-CC$_6$H$_4$Me-4)(CO)$_4$($\eta^5$-7,8-C$_2$B$_9$H$_{11}$)($\eta^5$-C$_5$H$_5$)] (**2b**)[c] | red | | 2048 s, 2014 m, 1982 m, 1942 w | | |
| [WR(CO)$_4${$\sigma$,$\eta^5$-9-CH(C$_6$H$_4$Me-4)-7,8-C$_2$B$_9$H$_{10}$}($\eta^5$-C$_5$H$_5$)] (**3a**) | green | 45 | 2026 s, 1983 m, 1941 s, 1866 m | 32.1 (32.7) | 3.3 (3.3) |
| [MoRu(CO)$_4${$\sigma$,$\eta^5$-9-CH(C$_6$H$_4$Me-4)-7,8-C$_2$B$_9$H$_{10}$}($\eta^5$-C$_5$H$_5$)] (**3b**) | green | 43 | 2022 s, 1978 m, 1950 m, 1878 m | 37.2 (37.4) | 4.2 (3.8) |
| [WRuO{$\mu$-$\sigma$,$\eta^5$-9-CH(C$_6$H$_4$Me-4)-7,8-C$_2$B$_9$H$_{10}$}(CO)$_2$($\eta^5$-C$_5$H$_5$)] (**4a**) | purple | 5 | 2020 s, 1970 s | 32.0 (31.1) | 4.5 (3.5) |
| [WRuO{$\mu$-$\sigma$,$\eta^5$-7,8-Me$_2$-10-CH(C$_6$H$_4$Me-4)-7,8-C$_2$B$_9$H$_8$}(CO)$_2$-($\eta^5$-C$_5$H$_5$)] (**4b**) | red | 11 | 2008 s, 1958 s | 33.3 (33.1) | 4.1 (4.0) |
| [WRuO{$\mu$-$\sigma$,$\eta^5$-7,8-Me$_2$-9-CH(C$_6$H$_4$Me-2)-7,8-C$_2$B$_9$H$_8$}(CO)$_2$-($\eta^5$-C$_5$H$_5$)] (**4c**)[d] | red | 2 | 2010 s, 1960 s | | |
| [WR(CO)$_4${$\eta^5$-9-CH(PMe$_3$)(C$_6$H$_4$Me-4)-7,8-C$_2$B$_9$H$_{10}$}-($\eta^5$-C$_5$H$_5$)] (**5a**) | red | 81 | 1976 s, 1906 s, 1826 w | 34.2 (34.2) | 4.1 (4.2) |
| [MoR(CO)$_4${$\eta^5$-9-CH(PMe$_3$)(C$_6$H$_4$Me-4)-7,8-C$_2$B$_9$H$_{10}$}-($\eta^5$-C$_5$H$_5$)] (**5b**) | red | 71 | 1978 s, 1910 s, 1836 w | 37.9 (38.5) | 4.7 (4.7) |
| [WRu($\mu$-H){$\mu$-$\eta^5$,$\eta'^5$-7,8-Me$_2$-9-C$_5$H$_4$-10-CH$_2$(C$_6$H$_4$Me-4)-7,8-C$_2$B$_9$H$_7$}(CO)$_5$] (**6a**)[e] | red | 5 | 2058 s, 2032 w, 2008 m, 1966 w, 1940 m | | |
| [MoRu($\mu$-H){$\mu$-$\eta^5$,$\eta'^5$-7,8-Me$_2$-9-C$_5$H$_4$-10-CH$_2$(C$_6$H$_4$Me-4)-7,8-C$_2$B$_9$H$_7$}(CO)$_5$] (**6b**) | red | 69 | 2058 s, 2034 w, 2006 m, 1980 w, 1952 m | 39.8 (39.7) | 3.8 (4.1) |
| [MoRu($\mu$-H){$\mu$-$\eta^5$,$\eta'^5$-7,8-Me$_2$-9-C$_5$H$_4$-10-CH$_2$(C$_6$H$_4$Me-2)-7,8-C$_2$B$_9$H$_7$}(CO)$_5$] (**6c**) | red | 22 | 2058 s, 2036 w, 2006 m, 1980 w, 1954 m | 44.3 (44.0) | 5.1 (5.3)[f] |
| [WRu($\mu$-H){$\mu$-$\eta^5$,$\eta'^5$-9-C$_5$H$_4$-10-CH$_2$(C$_6$H$_4$Me-4)-7,8-C$_2$B$_9$H$_9$}-(CO)$_5$] (**6d**)[g] | red | | 2058 s, 2030 w, 2004 m, 1960 w, 1942 m | | |
| [MoRu($\mu$-H){$\mu$-$\eta^5$,$\eta'^5$-9-C$_5$H$_4$-10-CH$_2$(C$_6$H$_4$Me-4)-7,8-C$_2$B$_9$H$_9$}-(CO)$_5$] (**6e**)[g] | red | | 2058 s, 2034 w, 2002 m, 1978 w, 1952 w | | |
| [WRu{$\mu$-$\sigma$,$\eta^5$-2,7-Me$_2$-8-CH$_2$(C$_6$H$_4$Me-4)-9-C(H)O-2,7-C$_2$B$_9$H$_6$}-(CO)$_4$($\eta^5$-C$_5$H$_5$)] (**7a**) | red | 30 | 2014 m, 1972 s, 1928 m | 34.9 (35.1) | 3.6 (3.6) |
| [WRu{$\mu$-$\sigma$,$\eta^5$-2,7-Me$_2$-8-CH$_2$(C$_6$H$_4$Me-2)-9-C(H)O-2,7-C$_2$B$_9$H$_6$}-(CO)$_4$($\eta^5$-C$_5$H$_5$)] (**7b**) | red | 6 | 2014 m, 1972 s, 1954 m | 35.1 (35.1) | 3.4 (3.6) |

[a] Measured in $CH_2Cl_2$; broad medium-intensity bands observed at ca. 2550 cm$^{-1}$ in the spectra of all of the compounds are due to B−H absorptions. [b] Calculated values are given in parentheses. [c] Complex isomerizes rapidly into **3b**. [d] Complex **4c** forms with **4d** in small amounts as an inseparable isomeric mixture, see text. [e] Complex difficult to obtain free of **7a**; therefore, microanalytical data not available, see text. [f] Crystallizes with one molecule of pentane. [g] Complex forms in trace amounts, identified spectroscopically, see text.



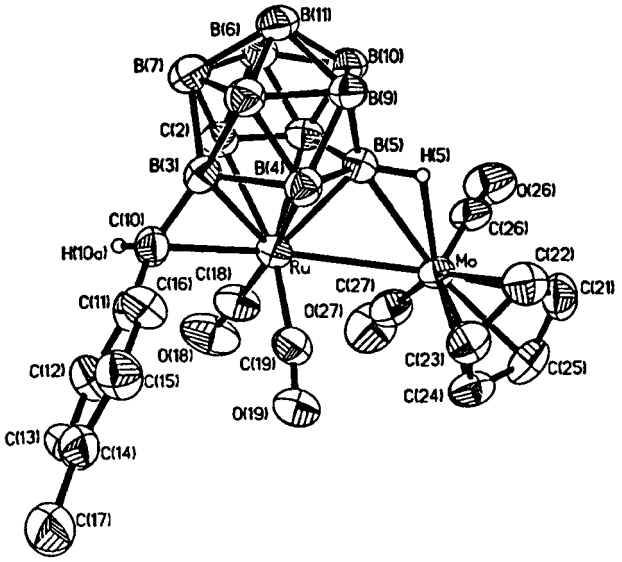


**Figure 1.** Molecular structure of [MoRu(CO)$_4${$\sigma$,$\eta^5$-9-CH(C$_6$H$_4$Me-4)-7,8-C$_2$B$_9$H$_{10}$}($\eta^5$-C$_5$H$_5$)] (**3b**) showing the crystallographic labeling scheme. Except for H(5) and H(10a), hydrogen atoms are omitted for clarity. Thermal ellipsoids are shown at 50% probability level.

site forms the agostic B(5)−H(5)⇀Mo linkage. Numerous dimetal complexes are known with a *closo*-3,1,2-MC$_2$B$_9$ icosahedral framework linked to a second metal−ligand fragment M′L$_n$ by a metal−metal bond and by either a B$_\alpha$−H → M′ or a B$_\beta$−H⇀M′ linkage.[6] The dimetal complexes **3** are electronically saturated with 34 valence electrons. The 9-CH(C$_6$H$_4$Me-4)-7,8-C$_2$B$_9$H$_{10}$ cage system formally contributes 7 electrons to the 27-electron (OC)$_2$RuM(CO)$_2$($\eta^5$-C$_5$H$_5$) (M = Mo or W) fragments.

The spectroscopic data for the complexes **3** are in agreement with the results of the X-ray diffraction study of **3b**. In the IR spectra (Table 1), there are four CO stretching bands for each of these asymmetric molecules. The presence of the ubiquitous B−H⇀Mo group in **3b** is revealed in the $^1$H NMR spectrum by a quartet resonance at $\delta$ −13.25 ($J$(BH) = 82 Hz) and in the $^{11}$B-{$^1$H} NMR spectrum by a singlet at $\delta$ 22.4 of relative intensity corresponding to one boron nucleus. This singlet resonance, as expected,[6] became a doublet in a proton-coupled $^{11}$B spectrum ($J$(HB) = 82 Hz). A further singlet signal at $\delta$ 3.5 is assigned to the B($\mu$-C)Ru group, as it remains a singlet in the fully coupled $^{11}$B spectrum. In the $^1$H NMR spectrum, the non-equivalent cage CH groups of the unsymmetrical structure display peaks at $\delta$ 2.49 and 3.55. The resonance for the C*H*(C$_6$H$_4$Me-4) proton of the bridge system is observed at $\delta$ 6.04.[11,12] The $^{13}$C{$^1$H} NMR spectrum showed four CO resonances (Table 2), in accord with the asymmetric structure. Signals for the cage CH groups occur at $\delta$ 46.7 and 53.6, and a very broad peak at $\delta$ 77.2 is characteristic for the B*C*(H)C$_6$H$_4$Me-4 nucleus.[11−13] The NMR data for **3a** are similar.

The syntheses of the complexes **3** were accompanied by the formation of minor products, identified spectroscopically, as described later, but formed in such small quantities that they could not all be fully characterized. However, one minor product that was fully characterized was the oxo−tungsten complex [WRuO{$\mu$-$\sigma$,$\eta^5$-9-CH(C$_6$H$_4$Me-4)-7,8-C$_2$B$_9$H$_{10}$}(CO)$_2$($\eta^5$-C$_5$H$_5$)] (**4a**), the formulation of which became apparent following an X-ray diffraction study. It seems likely that it is produced directly from **2a** over the time period required for formation of **3a** rather than *via* the latter as an intermediate. Thus, attempts to produce **4a** by treating **3a** with $H_2O_2$ solutions, or by stirring $CH_2Cl_2$ solutions

**Table 2. $^{1}H$, $^{13}C$, and $^{11}B$ NMR Data[a]**

| compd | $^{1}H/\delta$[b] | $^{13}C/\delta$[c] | $^{11}B/\delta$[d] |
|---|---|---|---|
| **2a** | 2.00 (s, 2 H, cage CH), 2.35 (s, 3 H, Me-4), 5.80 (s, 5 H, $C_5H_5$), 7.18 (s, 4 H, $C_6H_4$) | 301.9 ($\mu$-C), 211.9 (br, CO), 153.0, 140.8, 129.6, 128.1 ($C_6H_4$), 93.1 ($C_5H_5$), 41.9 (cage CH), 21.5 (Me-4) | 3.2 (1 B), −0.9 (1 B), −5.2 (4 B), −9.1 (1 B), −17.8 (2 B) |
| **2b**[e] | 2.08 (s, 2 H, cage CH), 2.37 (s, 3 H, Me-4), 5.72 (s, 5 H, $C_5H_5$), 7.21 (s, 4 H, $C_6H_4$) | | 4.8 (1 B), −0.2 (1 B), −4.8 (4 B), −8.6 (1 B), −17.6 (2 B) |
| **3a** | −14.10 (br q, 1 H, B−H⇀W, $J$(BH) = 79), 2.30 (s, 3 H, Me-4), 2.55, 3.65 (s × 2, 2 H, cage CH), 5.58 (s, 5 H, $C_5H_5$), 6.11 (s, 1 H, $\mu$-CH), 7.09, 7.37 ($(AB)_2$, 4 H, $C_6H_4$, $J$(AB) = 8) | 231.9, 226.1 (WCO), 196.6, 195.7 (RuCO), 139.1, 138.5, 130.8, 129.7, 129.1, 128.8 ($C_6H_4$), 92.9 ($C_5H_5$), 78.7 (vbr, $\mu$-CH), 56.5, 39.9 (cage CH), 21.5 (Me-4) | 26.0 (1 B, B−H⇀W, $J$(HB) = 79), 11.2 (1 B), 3.3 (2 B, B($\mu$-C)Ru and BH), −3.4 (1 B), −7.0 (1 B), −12.6 (1 B), −19.9 (2 B) |
| **3b** | −13.25 (br q, 1 H, B−H⇀Mo, $J$(BH) = 82), 2.29 (s, 3 H, Me-4), 2.49, 3.55 (s × 2, 2 H, cage CH), 5.45 (s, 5 H, $C_5H_5$), 6.04 (s, 1 H, $\mu$-CH), 7.08, 7.37 ($(AB)_2$, 4 H, $C_6H_4$, $J$(AB) = 8) | 245.2, 236.6 (MoCO), 199.1, 195.6 (RuCO), 139.1, 138.1, 130.6, 129.9, 129.6, 127.9 ($C_6H_4$), 94.5 ($C_5H_5$), 77.2 (vbr, $\mu$-CH), 53.6, 46.7 (cage CH), 21.4 (Me-4) | 22.4 (1 B, B−H⇀Mo, $J$(HB) = 82), 9.8 (1 B), 3.5 (1 B, B($\mu$-C)Ru), 2.2 (1 B), −4.0 (1 B), −7.4 (1 B), −12.6 (1 B), −20.6 (2 B) |
| **4a** | 2.38 (s, 3 H, Me-4), 2.44, 3.08 (s × 2, 2 H, cage CH), 6.25 (s, 5 H, $C_5H_5$), 6.58 ($(AB)_2$, 2 H, $C_6H_4$, $J$(AB) = 8), 6.87 (s, 1 H, $\mu$-CH), 7.11 ($(AB)_2$, 2 H, $C_6H_4$, $J$(AB) = 8) | 195.6, 192.0 (CO), 141.9, 138.6, 128.9, 126.2 ($C_6H_4$), 107.9 ($C_5H_5$), 54.5, 47.5 (cage CH), 20.9 (Me-4)[f] | 15.8 (1 B, B($\mu$-C)W), −1.7 (1 B), −5.9 (2 B), −9.1 (1 B), −11.5 (2 B), −20.1 (1 B), −24.8 (1 B) |
| **4b** | 2.21 (s, 3 H, Me-4), 2.36, 2.37 (s × 2, 6 H, cage Me), 6.25 (s, 5 H, $C_5H_5$), 6.71, 7.06 ($(AB)_2$, 4 H, $C_6H_4$, $J$(AB) = 8), 7.19 (s, 1 H, $\mu$-CH) | 196.7, 190.0 (CO), 151.0, 138.1, 128.2, 127.8 ($C_6H_4$), 108.3 ($C_5H_5$), 69.3, 65.6 (*C*Me), 31.3, 31.1 (C*Me*), 21.1 (Me-4)[f] | 21.0 (1 B, B($\mu$-C)W), −5.6 (2 B), −9.6 (3 B), −10.8 (1 B), −13.1 (1 B), −16.0 (1 B) |
| **4c**,**d**[g] | *2.20 (s, 3 H, Me-2), 2.21 (s, 3 H, Me-2), 2.22, 2.31 (s × 2, 6 H, cage Me), *2.35, *2.38 (s × 2, 6 H, cage Me), *6.14 (s, 5 H, $C_5H_5$), 6.48 (s, 5 H, $C_5H_5$), 6.90−7.80 (m, 8 H, $C_6H_4$), *7.34 (s, 1 H, $\mu$-CH), 7.82 (s, 1 H, $\mu$-CH) | | *21.0 (1 B, B($\mu$-C)W), 19.9 (1 B, B($\mu$-C)W), −3.6 (2 B), *−4.9 (2 B), −8.0 (2 B), −9.2 (1 B), *−10.3 (2 B), *−10.8 (1 B), −13.9 (1 B), *−16.0 (1 B) |
| **5a**[h] | −13.9 (br q, 1 H, B−H⇀W, $J$(BH) = 64), 1.78 (d, 9 H, MeP, $J$(PH) = 13), 2.12 (s, 1 H, cage CH), 2.34 (s, 3 H, Me-4), 2.58 (s, 1 H, cage CH), 3.48 (d, 1 H, CHP, $J$(PH) = 21), 5.48 (s, 5 H, $C_5H_5$), 6.92, 7.14, 7.27, 7.95 (d × 4, 4 H, $C_6H_4$, $J$(HH) = 8) | 228.0 (vbr, WCO), 207.3, 200.9 (RuCO), 137.9, 131.8, 130.1, 129.6, 129.2 ($C_6H_4$), 90.9 ($C_5H_5$), 38.1, 35.4 (cage CH), 21.0 (Me-4), 10.6 (d, MeP, $J$(PC) = 54)[f] | 22.6 (1 B, B−H⇀W, $J$(HB) = 64), −0.3 (1 B), −1.7 (1 B), −7.3 (1 B, BCH), −9.3 (1 B), −13.1 (1 B), −20.2 (2 B), −23.6 (1 B) |
| **5b**[i] | −13.3 (br q, 1 H, B−H⇀Mo, $J$(BH) = 61), 1.79 (d, 9 H, MeP, $J$(PH) = 13), 2.04 (s, 1 H, cage CH), 2.34 (s, 3 H, Me-4), 2.52 (s, 1 H, cage CH), 3.43 (d, 1 H, CHP, $J$(PH) = 21), 5.36 (s, 5 H, $C_5H_5$), 6.91, 7.14, 7.28, 7.93 (d × 4, 4 H, $C_6H_4$, $J$(HH) = 8) | 250.3, 237.8 (MoCO), 207.2, 201.2 (RuCO), 138.1, 132.0, 130.2 (2 C), 129.9, 129.2, 126.0 ($C_6H_4$), 92.5 ($C_5H_5$), 38.2, 35.5 (cage CH), 21.1 (Me-4), 10.7 (d, MeP, $J$(PC) = 55)[f] | 20.3 (1 B, B−H⇀Mo, $J$(HB) = 61), −1.6 (2 B), −7.3 (1 B, BCH), −9.6 (1 B), −13.4 (1 B), −19.8 (2 B), −23.6 (1 B) |
| **6a** | −18.94 (s, 1 H, $\mu$-H), 1.97 (s, 3 H, Me-4), 2.24 (s, 3 H, cage Me), 2.30 (br m, 2 H, $CH_2$), 2.38 (s, 3 H, cage Me), 5.06, 5.19 (m × 2, 2 H, $C_5H_4$), 5.80 (m, 2 H, $C_5H_4$), 6.80, 6.93 ($(AB)_2$, 4 H, $C_6H_4$, $J$(AB) = 8) | | 10.1 (1 B, $BCH_2$), 5.6 (1 B), −0.9 (1 B, $BC_5H_4$), −2.9 (2 B), −7.3 (1 B), −11.4 (2 B), −14.0 (1 B) |
| **6b** | −17.01 (s, 1 H, $\mu$-H), 1.59, 1.86 (d × 2, 1 H, $CH_2$, $J$(HH), = 15), 1.90 (s, 3 H, Me-4), 2.23, 2.42 (s × 2, 6 H, cage Me), 4.89, 5.02 (m × 2, 2 H, $C_5H_4$), 5.80 (m, 2 H, $C_5H_4$), 6.77, 6.92 ($(AB)_2$, 4 H, $C_6H_4$, $J$(AB) = 8) | 230.2, 222.7, 221.8 (MoCO), 196.6, 193.2 (RuCO), 142.0, 133.4, 129.3, 128.3 ($C_6H_4$), 95.9, 92.6, 92.1, 91.2 ($C_5H_4$), 75.0, 63.8 (*C*Me), 34.2, 31.0 (C*Me*), 30.2 (vbr, $BCH_2$), 20.9 (Me-4)[j] | 10.2 (1 B, $BCH_2$), 5.3 (1 B), −0.9 (1 B, $BC_5H_4$), −3.2 (2 B), −7.3 (1 B), −11.3 (2 B), −14.4 (1 B) |
| **6c** | −16.98 (s, 1 H, $\mu$-H), 1.43 (d, 1 H, $CH_2$, $J$(HH) = 17), 1.93 (s, 3 H, Me-2), 1.96 (d, 1 H, $CH_2$, $J$(HH) = 17), 2.15, 2.46 (s × 2, 6 H, cage Me), 4.91, 5.20, 5.76, 5.86 (m × 4, 4 H, $C_5H_4$), 6.78, 6.98 (m, 4 H, $C_6H_4$) | 230.1, 222.7, 221.1 (MoCO), 196.9, 192.9 (RuCO), 144.1, 136.0, 129.6, 129.2, 124.9, 124.1 ($C_6H_4$), 96.1, 92.0, 91.8 (1:1:2, $C_5H_4$), 75.2, 63.3 (*C*Me), 34.2, 31.0 (C*Me*), 26.5 (vbr, $BCH_2$), 20.7 (Me-2)[j] | 9.5 (1 B, $BCH_2$), 5.2 (1 B), −0.6 (1 B, $BC_5H_4$), −3.4 (2 B), −7.8 (1 B), −11.5 (2 B), −14.1 (1 B) |
| **6d**[k] | −17.55 (s, 1 H, $\mu$-H, $J$(WH) = 35), 2.25 (d, 1 H, $CH_2$, $J$(HH) = 16), 2.27 (s, 3 H, Me-4), 2.33 (d, 1 H, $CH_2$, $J$(HH) = 16), 2.70, 3.41 (s × 2, 2 H, cage CH), 4.78, 5.12, 5.62, 5.67 (m × 4, 4 H, $C_5H_4$), 6.84, 6.98 ($(AB)_2$, 4 H, $C_6H_4$, $J$(AB) = 8) | | |
| **6e**[k] | −16.21 (s, 1 H, $\mu$-H), 1.81, 1.95 (d × 2, 1 H, $CH_2$, $J$(HH) = 17), 2.25 (s, 3 H, Me-4), 3.80, 3.99 (s × 2, 2 H, cage CH), 4.81, 4.84, 5.63, 5.70 (m × 4, 4 H, $C_5H_4$), 6.82, 6.97 ($(AB)_2$, 4 H, $C_6H_4$, $J$(AB) = 8) | | |
| **7a** | 1.65 (s, 3 H, cage Me), 1.93 (s, 3 H, Me-4), 2.26 (s, 3 H, cage Me), 2.75, 2.90 (d × 2, 1 H, $CH_2$, $J$(HH) = 17), 5.79 (s, 5 H, $C_5H_5$), 7.03, 7.09 ($(AB)_2$, 4 H, $C_6H_4$, $J$(AB) = 8), 10.49 (s br, 1 H, BC(H)O) | 250.2 (br, C(H)O), 219.0, 208.3 (WCO), 203.6, 198.0 (RuCO), 140.6, 134.4, 129.6, 129.0 ($C_6H_4$), 92.6 ($C_5H_5$), 63.2, 61.8 (*C*Me), 31.5 (C*Me*), 28.8 (vbr, $BCH_2$), 23.3 (C*Me*), 20.8 (Me-4) | 57.6 (1 B, BW), 0.5 (1 B, $BCH_2$), −0.9 (1 B), −6.4 (2 B), −9.3 (1 B, BC(H)O), −11.7 (1 B), −17.5 (1 B), −19.0 (1 B) |
| **7b** | 1.92 (s, 3 H, Me-2), 2.06, 2.49 (s × 2, 6 H, cage Me), 2.75, 2.85 (d × 2, 1 H, $CH_2$, $J$(HH) = 17), 5.73 (s, 5 H, $C_5H_5$), 6.90−7.13 (m, 4 H, $C_6H_4$), 10.46 (br s, 1 H, BC(H)O) | 250.6 (br, C(H)O), 219.1, 208.3 (WCO), 202.7, 198.0 (RuCO), 144.5, 136.4, 130.9, 129.0, 126.0, 125.1 ($C_6H_4$), 93.1 ($C_5H_5$), 63.5, 62.4 (*C*Me), 31.7 (C*Me*), 24.8 (vbr, $BCH_2$), 23.5 (C*Me*), 21.1 (Me-2) | 57.9 (1 B, BW), 1.2 (1 B, $BCH_2$), −1.6 (1 B), −6.5 (2 B), −10.0 (1 B, BC(H)O), −12.8 (1 B), −17.3 (1 B), −18.9 (1 B) |

[a] Chemical shifts ($\delta$) in ppm; coupling constants ($J$) in Hertz; measurements in $CD_2Cl_2$. [b] Resonances for terminal BH protons occur as broad unresolved signals in the range of $\delta$ ca. −2 to 3. [c] $^{1}H$-decoupled; chemical shifts are positive to high frequency of $SiMe_4$. [d] $^{1}H$-decoupled; chemical shifts are positive to high frequency of $BF_3{\cdot}OEt_2$ (external). [e] Complex isomerizes too quickly for $^{13}C\{^{1}H\}$ NMR spectrum to be measured, see text. [f] Signal for *C*$HC_6H_4Me$ was not observed due to broadening by $^{11}B$ nuclei. [g] On the basis of relative peak intensities, the complex formed as a ca. 3:2 mixture of two isomers. Resonances due to minor isomer **4d** indicated with an asterisk. [h] $^{31}P\{^{1}H\}$ NMR: $\delta$ = 27.3. [i] $^{31}P\{^{1}H\}$ NMR: $\delta$ = 27.3. [j] Signal for B*C*($C_5H_4$) nucleus not observed due to broadening by $^{11}B$ nuclei, see text. [k] Only $^{1}H$ NMR spectrum measured as complex forms in trace amounts, see text.

**Table 3. Selected Internuclear Distances (Å) and Angles (deg) for [MoRu(CO)$_4${$\sigma$,$\eta^5$-9-CH(C$_6$H$_4$Me-4)-7,8-C$_2$B$_9$H$_{10}$}($\eta^5$-C$_5$H$_5$)] (3b), with Estimated Standard Deviations in Parentheses**

| | | | | | | | |
|---|---|---|---|---|---|---|---|
| Ru−C(1) | 2.309(4) | Ru−C(2) | 2.245(4) | Ru−B(3) | 2.166(4) | Ru−B(4) | 2.255(5) |
| Ru−B(5) | 2.198(5) | Ru−C(10) | 2.351(4) | Ru−C(18) | 1.908(4) | Ru−C(19) | 1.851(4) |
| Ru−Mo | 2.976(1) | B(3)−C(10) | 1.512(6) | B(5)−H(5) | 1.15 | B(5)−Mo | 2.486(5) |
| Mo−C(21) | 2.311(4) | Mo−C(22) | 2.358(4) | Mo−C(23) | 2.354(4) | Mo−C(24) | 2.287(4) |
| Mo−C(25) | 2.295(4) | Mo−C(26) | 1.919(4) | Mo−C(27) | 1.938(4) | Mo−H(5) | 1.83 |
| B(3)−Ru−C(10) | 38.8(2) | B(5)−Ru−Mo | 55.0(1) | C(10)−Ru−C(18) | 93.6(2) | C(10)−Ru−Mo | 157.6(1) |
| B(5)−Mo−Ru | 46.4(1) | Ru−Mo−C(26) | 113.8(1) | B(5)−H(5)−Mo | 111.2(1) | B(3)−C(10)−Ru | 64.0(2) |
| C(11)−C(10)−Ru | 117.9(3) | Ru−C(18)−O(18) | 173.4(4) | Ru−C(19)−O(19) | 173.0(4) | Mo−C(26)−O(26) | 176.6(3) |
| Mo−C(27)−O(27) | 174.3(4) | | | | | | |

**Table 4. Selected Internuclear Distances (Å) and Angles (deg) for [WRuO{$\mu$-$\sigma$,$\eta^5$-9-CH(C$_6$H$_4$Me-4)-7,8-C$_2$B$_9$H$_{10}$}(CO)$_2$($\eta^5$-C$_5$H$_5$)] (4a), with Estimated Standard Deviations in Parentheses**

| | | | | | | | |
|---|---|---|---|---|---|---|---|
| Ru−C(1) | 2.251(6) | Ru−C(2) | 2.265(7) | Ru−B(3) | 2.315(9) | Ru−B(4) | 2.310(8) |
| Ru−B(5) | 2.290(7) | Ru−C(5) | 1.898(8) | Ru−C(6) | 1.863(7) | Ru−W | 2.514(1) |
| C(1)−C(2) | 1.650 (9) | C(1)−B(5) | 1.78(1) | C(1)−B(6) | 1.73(1) | C(1)−B(10) | 1.72(1) |
| C(2)−B(3) | 1.72(1) | C(2)−B(6) | 1.71(1) | C(2)−B(7) | 1.71(1) | B(3)−B(4) | 1.84(1) |
| B(3)−B(7) | 1.81(1) | B(3)−B(8) | 1.78(1) | B(4)−B(5) | 1.85(1) | B(4)−B(8) | 1.80(1) |
| B(4)−B(9) | 1.78(1) | B(5)−B(9) | 1.77(1) | B(5)−B(10) | 1.83(1) | B(5)−C(10) | 1.62(1) |
| B(5)−W | 2.565(8) | B(6)−B(7) | 1.74(1) | B(6)−B(10) | 1.78(1) | B(6)−B(11) | 1.77(1) |
| B(7)−B(8) | 1.78(1) | B(7)−B(11) | 1.73(1) | B(8)−B(9) | 1.82(1) | B(8)−B(11) | 1.76(1) |
| B(9)−B(10) | 1.74(1) | B(9)−B(11) | 1.79(1) | B(10)−B(11) | 1.77(1) | C(5)−O(5) | 1.166(9) |
| C(6)−O(6) | 1.145(9) | C(10)−H(10A) | 0.96 | C(10)−C(11) | 1.513(8) | C(10)−W | 2.082(6) |
| C(11)−C(12) | 1.357(9) | C(11)−C(16) | 1.400(9) | C(12)−C(13) | 1.422(9) | C(13)−C(14) | 1.37(1) |
| C(14)−C(15) | 1.37(1) | C(14)−C(17) | 1.51(9) | C(15)−C(16) | 1.394(9) | W−C(21) | 2.46(1) |
| W−C(22) | 2.440(9) | W−C(23) | 2.304(9) | W−C(24) | 2.33(1) | W−C(25) | 2.378(9) |
| W−O(1) | 1.716(5) | C(21)−C(22) | 1.31(1) | C(21)−C(25) | 1.36(2) | C(22)−C(23) | 1.39(1) |
| C(23)−C(24) | 1.44(1) | C(24)−C(25) | 1.37(2) | | | | |
| C(5)−Ru−C(6) | 92.1(3) | C(5)−Ru−W | 101.3(2) | C(6)−Ru−W | 87.0(2) | Ru−B(5)−W | 62.1(2) |
| C(10)−B(5)−W | 54.1(3) | Ru−C(5)−O(5) | 178.1(7) | Ru−C(6)−O(6) | 175.7(7) | B(5)−C(10)−H(10A) | 103.9(4) |
| B(5)−C(10)−C(11) | 125.3(5) | H(10A)−C(10)−C(11) | 104.0(3) | B(5)−C(10)−W | 86.9(3) | H(10A)−C(10)−W | 104.2(2) |
| C(11)−C(10)−W | 129.0(5) | Ru−W−B(5) | 53.6(2) | Ru−W−C(10) | 92.3(2) | B(5)−W−C(10) | 38.9(2) |
| Ru−W−O(1) | 105.2(2) | B(5)−W−O(1) | 106.9(2) | C(10)−W−O(1) | 103.2(2) | | |

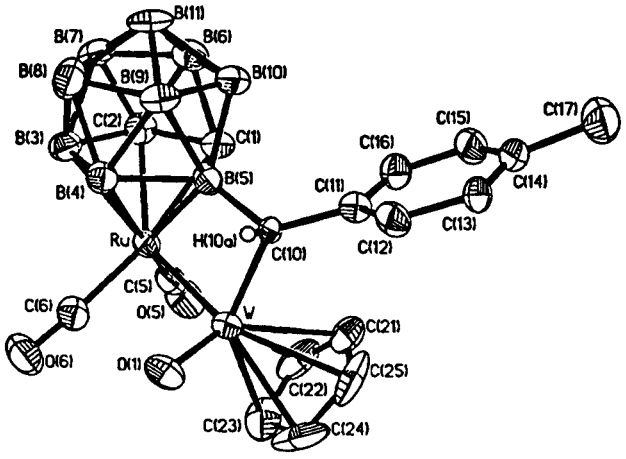


**Figure 2.** Molecular structure of [WRuO{$\mu$-$\sigma$,$\eta^5$-9-CH(C$_6$H$_4$-Me-4)-7,8-C$_2$B$_9$H$_{10}$}(CO)$_2$($\eta^5$-C$_5$H$_5$)] (**4a**) showing the crystallographic labeling scheme. Except for H(10a), hydrogen atoms are omitted for clarity. Thermal ellipsoids are shown at 50% probability level.

of **3a** in moist air rather than under nitrogen, did not yield the oxo complex. No similar oxo−molybdenum species was observed in the formation of **3b** from **2b**.

The molecule **4a** is shown in Figure 2, and salient bond distances and angles are listed in Table 4. The Ru atom is coordinated by two terminally bound CO molecules and interacts with the open $C_2B_3$ face of the cage in the usual pentahapto manner.[3] The W atom carries the $\eta^5$-$C_5H_5$ ring and the oxygen atom (W−O(1) = 1.716(5) Å) and forms a bridge to the cage atom B(5) through C(10) (W−C(10) = 2.082(6) Å, C(10)−B(5) = 1.62(1) Å). The W−O(1) separation may be compared with that in [W$_2$O($\mu$-CC$_6$H$_4$Me-4)(CO)$_2$($\eta^5$-7,8-Me$_2$-7,8-C$_2$B$_9$H$_9$)($\eta^5$-C$_9$H$_7$)] (C$_9$H$_7$ = indenyl, 1.699(6) Å),[14a] [W$_2$-FeO{$\mu_3$-C$_2$(C$_6$H$_4$Me-4)$_2$}(CO)$_5$($\eta^5$-C$_5$H$_5$)$_2$] (1.726(7) Å),[14b] or [WRe$_2$O{$\mu_3$-C≡CC(Me)=CH$_2$}(CO)$_8$($\eta^5$-C$_5$Me$_5$)] (1.699(6) Å).[15] Interestingly, the W−O(1) distance is very close to the mean value (1.711 Å) found for W−O bonds in many oxo−tungsten species where it has been demonstrated that such distances cannot be utilized to identify bond multiplicity.[16] However, if it is assumed there is a W=O bond in **4a**, the molecule is electronically unsaturated, having 30 rather than 34 cluster valence electrons. The short Ru−W distance (2.514(1) Å) is in accord with the electronic unsaturation. This bond length may be compared with the appreciably longer Ru−W distances in [WRu($\mu$-CC$_6$H$_4$Me-4)(CO)$_3$($\eta^5$-7,8-Me$_2$-7,8-C$_2$B$_9$H$_9$)($\eta^5$-C$_5$H$_5$)] (2.803(2) Å),[17] [WRu($\mu$-Cl)-($\mu$-CMe)(CO)$_2$(PPh$_3$)($\eta^5$-C$_5$H$_5$)] (2.769(1) Å),[18] and [W$_2$-Ru($\mu_3$-MeC≡CMe)(CO)$_7$($\eta^5$-C$_5$H$_5$)$_2$] (2.835(2)−3.026(1) Å),[18] where the metal centers have filled 18-electron valence shells. Even in the 60-electron unsaturated cluster [W$_3$Ru($\mu$-CO)($\mu_3$-$\eta^2$-CO)($\mu$-CPh)$_2$($\mu_3$-CPh)(CO)$_2$-($\eta^5$-C$_5$H$_5$)$_3$],[19] all three W−Ru separations are significantly longer (2.735(2)−2.847(2) Å) than that found in

(14) (a) Howard, J. A. K.; James, A. P.; Jelfs, A. N. de M.; Nunn, C. M.; Stone, F. G. A. *J. Chem. Soc., Dalton Trans.* **1987**, 1221. (b) Busetto, L.; Jeffery, J. C.; Mills, R. M.; Stone, F. G. A.; Went, M. J.; Woodward, P. *J. Chem. Soc., Dalton Trans.* **1983**, 101.

(15) Chi, Y.; Cheng, P-S.; Wu, H-L.; Hwang, D-K.; Su, P-C.; Peng, S-M.; Lee, G-H. *J. Chem. Soc., Chem. Commun.* **1994**, 1839.

(16) Mayer, J. M. *Inorg. Chem.* **1988**, *27*, 3899.

(17) Green, M.; Howard, J. A. K.; Jelfs, A. N. de M.; Johnson, O.; Stone, F. G. A. *J. Chem. Soc., Dalton Trans.* **1987**, 73.

(18) Howard, J. A. K.; Laurie, J. C. V.; Johnson, O.; Stone, F. G. A. *J. Chem. Soc., Dalton Trans.* **1985**, 2017.

(19) Farrugia, L. J.; Jeffery, J. C.; Marsden, C.; Sherwood, P; Stone, F. G. A. *J. Chem. Soc., Dalton Trans.* **1987**, 51.

**4a**. For electron counting purposes, in the formulation of the latter it is assumed that the metal−metal bond is multiple in character.

The nonspectator behavior of *nido*-$C_2B_9$ cages when pentahapto-coordinated to metal centers is generally associated with reactions at BH groups located either at the CC*B*BB or at the CCB*B*B sites of the ligating rings.[6] Products formed resulting from the nonspectator behavior of the carborane fragment, when $\eta^5$-7,8-$C_2B_9H_{11}$ cages are ligands, usually result from activation of $B_\alpha$ sites, presumably for statistical reasons. However, with $\eta^5$-7,8-$Me_2$-7,8-$C_2B_9H_9$ ligands, the structures of the complexes obtained reveal that it is more usually the B−H bond at the $B_\beta$ site which has undergone activation. In agreement with this behavioral pattern the CH($C_6H_4$Me-4) fragment in **4a** is attached to B(5), an α site in the CC*B*BB ring coordinated to the ruthenium. In contrast, in the complexes [MoW{$\mu$-$\sigma$,$\eta^3$-7,8-$Me_2$-10-CH($C_6H_4$Me-4)-7,8-$C_2B_9H_8$}(CO)$_3$(EtC≡CEt)($\eta^5$-$C_9H_7$)][20] and [WRu{$\mu$-$\sigma$,$\eta^5$-7,8-$Me_2$-10-CH($C_6H_4$Me-4)-7,8-$C_2B_9H_8$}(CO)$_3$($PMe_3$)($\eta^5$-$C_5H_5$)],[17] species with Me substituents on the cage carbons and also with CH($C_6H_4$Me-4) groups linking their *nido*-$C_2B_9$ cages to the exopolyhedral metal centers, it is the boron atom in the $\beta$ site in the CCB*B*B rings which forms the bridge.

The structure of **4a** also differs from that of [MoW{$\mu$-$\sigma$,$\eta^3$-7,8-$Me_2$-10-CH($C_6H_4$Me-4)-7,8-$C_2B_9H_8$}(CO)$_3$(EtC≡CEt)($\eta^5$-$C_9H_7$)] in that in the latter molecule the open face of the CCBBB ring has a pronounced slippage, the cage C−W ring distances being ca. 3.04 Å. Hence, the cage is trihapto-bonded to the tungsten center via the boron atoms in the $C_2B_3$ ring,[20] whereas in **4a**, the cage C−Ru separations (2.251(6) and 2.265(7) Å) are typical of those found in other *closo*-3,1,2-$RuC_2B_9$ structures.[3]

The formation of oxo complexes like **4a** has been observed to occur readily with related systems. Thus, [$W_2$O($\mu$-CC$_6$H$_4$Me-4)(CO)$_2$($\eta^5$-7,8-$Me_2$-7,8-$C_2B_9H_9$)($\eta^5$-$C_9H_7$)] is formed by treating the bridged alkylidyne−ditungsten complex [$W_2$($\mu$-CC$_6$H$_4$Me-4)(CO)$_3$($\eta^5$-7,8-$Me_2$-7,8-$C_2B_9H_9$)($\eta^5$-$C_9H_7$)] with aqueous $H_2O_2$,[14a] and [$W_2$FeO{$\mu_3$-$C_2$($C_6H_4$Me-4)$_2$}(CO)$_5$($\eta^5$-$C_5H_5$)$_2$] forms from the alkyne complex [$W_2$Fe{$\mu_3$-$C_2$($C_6H_4$Me-4)$_2$}(CO)$_6$($\eta^5$-$C_5H_5$)$_2$] when the latter is placed in contact with moist air.[14b] It has also been shown that the mixed-metal fulvalene complex [MoRu($\mu$-$\eta^5$,$\eta'^5$-$C_5H_4$−$C_5H_4$)(CO)$_5$] reacts with PhC≡CPh to give an oxo−molybdenum species [MoRuO($\mu$-$\eta^5$,$\eta'^5$-$C_5H_4$−$C_5H_4$)($\mu$-PhC≡CPh)(CO)$_2$], with the source of the oxo group in this process also being attributed to moisture possibly derived from the glassware.[21a]

The NMR data for **4a** (Table 2) are in accord with the structure established by X-ray diffraction. In the $^1$H NMR spectrum, the nonequivalent cage CH groups are seen as two signals at $\delta$ 2.44 and 3.08, while a singlet resonance at $\delta$ 6.87 may be attributed to the $\mu$-CH proton. In the spectrum of [WRu{$\mu$-$\sigma$,$\eta^5$-7,8-$Me_2$-10-CH($C_6H_4$Me-4)-7,8-$C_2B_9H_8$}(CO)$_3$($PMe_3$)($\eta^5$-$C_5H_5$)], the corresponding resonance is at $\delta$ 5.95, although in this molecule the CH($C_6H_4$Me-4) group is $\sigma$ bonded to the ruthenium atom and the tungsten-pentacoordinated by the cage,[17] the opposite to the arrangement in **4a**. In the $^{13}$C{$^1$H} NMR spectrum of the latter, diagnostic peaks for the cage carbon nuclei are seen at $\delta$ 47.5 and 54.5.[6b] A peak for the *C*H($C_6H_4$Me-4) nucleus was not observed, but this is not unusual as such resonances are often broad due to the quadrupolar effect of the adjacent $^{11}$B nuclei and are, thus, lost in the noise unless a strong solution can be measured. The $^{11}$B{$^1$H} NMR spectrum revealed a diagnostic resonance for the *B*C(H)$C_6H_4$Me-4 nucleus at $\delta$ 15.8, which remained as a singlet in a fully coupled $^{11}$B spectrum, whereas the other peaks became doublets.[6b]

The complexes **3** were treated with 1 mol equiv of $PMe_3$ to determine if one of the terminal CO ligands would be substituted without disrupting the overall structures or alternatively whether the phosphine would attack the carbon atom of the bridging CH($C_6H_4$Me-4) group. It has been previously observed that tertiary phosphines react with the compound [Rh(CO)($PPh_3$){$\sigma$,$\eta^5$-10-CH($C_6H_4$Me-4)-7,9-$C_2B_9H_{10}$}] to yield the ylid complexes [Rh(CO)($PPh_3$){$\eta^5$-10-CH($PR_3$)($C_6H_4$Me-4)-7,9-$C_2B_9H_{10}$}].[22] Reactions of the molecules **3** with $PMe_3$ proceeded smoothly to afford the zwitterionic complexes [MRu(CO)$_4$){$\eta^5$-9-CH($PMe_3$)($C_6H_4$Me-4)-7,8-$C_2B_9H_{10}$}($\eta^5$-$C_5H_5$)] (M = W (**5a**), Mo (**5b**)). This was indicated by their NMR spectra and confirmed for **5a** by an X-ray diffraction study. The results of the latter are given in Table 5, and the molecule is shown in Figure 3.

The W−Ru bond (2.921(1) Å) is bridged by the 9-CH($PMe_3$)($C_6H_4$Me-4)-7,8-$C_2B_9H_{10}$ cage system with the open CCBBB face of the *nido*-$C_2B_9$ framework pentacoordinated to the ruthenium and with an exopolyhedral $B_\alpha$−H⇀W bond. The atom H(5) was located and its position refined (B(5)−W = 2.436(6) Å, B(5)−Ru = 2.176(6) Å, B(5)−H(5) = 1.44(10) Å, W−H(5) = 1.78 (10) Å). The atom B(3) carries the CH($PMe_3$)($C_6H_4$Me-4) substituent (B(3)−C(20) = 1.650(8) Å). Each metal center is coordinated by two CO molecules with one molecule C(43)O(43) linearly bound (Ru−C(43)−O(43) = 179.5(5)°) and with the others showing slight deviations from linearity (Ru−C(44)−O(44) = 174.8(5)°, W−C(41)−O(41) = 172.9(5)°, W−C(42)−O(42) = 176.4(6)°). The conversion of **3a** into **5a**, thus, involved cleavage of the bond between the Ru atom and the CH($C_6H_4$Me-4) group.

The NMR data for the complexes **5** are in accord with the results of the X-ray study on **5a**. Thus, in the $^1$H NMR spectrum of the latter, there is a broad quartet at $\delta$ −13.9 ($J$(BH) = 64 Hz) characteristic of the B−H⇀W group. In the proton-coupled $^{11}$B NMR spectrum, there is a doublet resonance for this group at $\delta$ 22.6 ($J$(HB) = 64 Hz). The other doublet signals in the fully coupled spectrum have the customary $^1$H−$^{11}$B couplings in the range 100−140 Hz. A resonance which appeared as a singlet in the $^{11}$B NMR spectrum at $\delta$ −7.3 may be assigned to the boron atom attached to the exopolyhedral CH($PMe_3$)($C_6H_4$Me-4) moiety, the $PMe_3$ group of which displays a peak at $\delta$ 27.3 in the $^{31}$P{$^1$H}

(20) Green, M.; Howard, J. A. K.; James, A. P.; Jelfs, A. N. de M.; Nunn, C. M.; Stone, F. G. A. *J. Chem. Soc., Chem. Commun.* **1985**, 1778.

(21) (a) Drage, J. S.; Tilset, M.; Vollhardt, K. P. C.; Weidman, T. W. *Organometallics* **1984**, *3*, 812. (b) Vollhardt, K. P. C.; Weidman, T. W. *Organometallics* **1984**, *3*, 82. (c) Boese, R.; Huffman, M. A.; Vollhardt, K. P. C. *Angew. Chem., Int. Ed. Engl.* **1991**, *30*, 1463.

(22) Goldberg, J. E.; Jeffery, J. C.; Stone, F. G. A. *J. Organomet. Chem.* **1993**, *462*, 353.

**Table 5. Selected Internuclear Distances (Å) and Angles (deg) for [WRu(CO)$_4${$\eta^5$-9-CH(PMe$_3$)(C$_6$H$_4$Me-4)-7,8-C$_2$B$_9$H$_{10}$}($\eta^5$-C$_5$H$_5$)] (5a), with Estimated Standard Deviations in Parentheses**

| | | | | | | | |
|---|---|---|---|---|---|---|---|
| W−C(42) | 1.953(6) | W−C(41) | 1.955(6) | W−C(12) | 2.293(6) | W−C(11) | 2.306(6) |
| W−C(13) | 2.331(6) | W−C(15) | 2.391(6) | W−C(14) | 2.400(6) | W−B(5) | 2.436(6) |
| W−Ru | 2.921(1) | W−H(5) | 1.78(10) | Ru−C(43) | 1.851(6) | Ru−C(44) | 1.899(6) |
| Ru−B(5) | 2.176(6) | Ru−C(1) | 2.211(5) | Ru−C(2) | 2.269(5) | Ru−B(4) | 2.292(6) |
| Ru−B(3) | 2.315(6) | C(41)−O(41) | 1.160(8) | C(42)−O(42) | 1.157(8) | C(43)−O(43) | 1.150(7) |
| C(44)−O(44) | 1.149(7) | C(1)−C(2) | 1.631(7) | C(1)−B(10) | 1.698(8) | C(1)−B(6) | 1.711(8) |
| C(1)−B(5) | 1.731(8) | C(2)−B(7) | 1.708(8) | C(2)−B(3) | 1.715(8) | C(2)−B(6) | 1.733(8) |
| B(3)−C(20) | 1.650(8) | B(3)−B(8) | 1.798(8) | B(3)−B(7) | 1.809(8) | B(3)−B(4) | 1.838(8) |
| B(4)−B(8) | 1.781(8) | B(4)−B(9) | 1.801(8) | B(4)−B(5) | 1.805(8) | B(5)−B(9) | 1.780(9) |
| B(5)−B(10) | 1.810(9) | B(5)−H(5) | 1.44(10) | B(6)−B(7) | 1.752(9) | B(6)−B(10) | 1.762(9) |
| B(6)−B(11) | 1.766(9) | B(7)−B(8) | 1.763(9) | B(7)−B(11) | 1.775(9) | B(8)−B(9) | 1.787(9) |
| B(8)−B(11) | 1.800(9) | B(9)−B(10) | 1.783(9) | B(9)−B(11) | 1.789(9) | B(10)−B(11) | 1.754(9) |
| P−C(33) | 1.785(6) | P−C(32) | 1.793(7) | P−C(31) | 1.797(6) | P−C(20) | 1.811(5) |

| | | | | | |
|---|---|---|---|---|---|
| C(42)−W−C(41) | 75.3(3) | C(42)−W−B(5) | 99.6(2) | C(41)−W−B(5) | 109.1(2) |
| C(42)−W−Ru | 122.8(2) | C(41)−W−Ru | 76.7(2) | B(5)−W−Ru | 46.9(2) |
| C(43)−Ru−C(44) | 88.2(3) | C(43)−Ru−C(1) | 174.0(2) | C(44)−Ru−C(1) | 96.8(2) |
| C(43)−Ru−C(2) | 140.3(2) | C(44)−Ru−C(2) | 95.9(2) | C(1)−Ru−C(2) | 42.7(2) |
| C(43)−Ru−W | 88.7(2) | C(44)−Ru−W | 102.4(2) | C(1)−Ru−W | 86.9(1) |
| C(2)−Ru−W | 128.2(1) | O(41)−C(41)−W | 172.9(5) | O(42)−C(42)−W | 176.4(6) |
| O(43)−C(43)−Ru | 179.5(5) | O(44)−C(44)−Ru | 174.8(5) | C(33)−P−C(32) | 108.9(4) |
| C(33)−P−C(31) | 106.9(3) | C(32)−P−C(31) | 107.1(4) | C(33)−P−C(20) | 114.3(3) |
| C(32)−P−C(20) | 112.5(3) | C(31)−P−C(20) | 106.7(3) | C(21)−C(20)−B(3) | 116.6(4) |
| C(21)−C(20)−P | 108.8(4) | B(3)−C(20)−P | 120.5(4) | | |



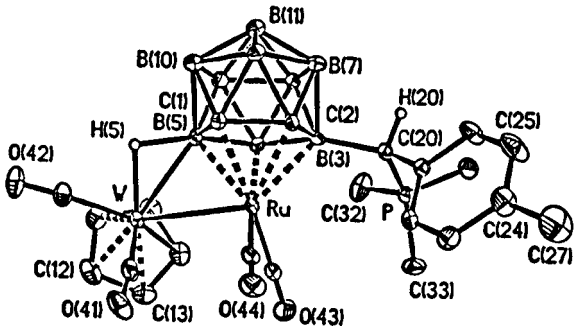


**Figure 3.** Molecular structure of [WRu(CO)$_4${$\eta^5$-9-CH(PMe$_3$)(C$_6$H$_4$Me-4)-7,8-C$_2$B$_9$H$_{10}$}($\eta^5$-C$_5$H$_5$)] (**5a**) showing the crystallographic labeling scheme. Except for H(5) and H(20), hydrogen atoms are omitted for clarity. Thermal ellipsoids are shown at 40% probability level.

NMR spectrum. The $^1$H NMR spectrum shows peaks for the nonequivalent cage CH groups at $\delta$ 2.12 and 2.58, and a doublet at $\delta$ 3.48 ($J$(PH) = 21 Hz) may be assigned to the proton of the C*H*(PMe$_3$) group. Interestingly, four distinct doublets are observed for the C$_6$H$_4$ protons, indicating restricted rotation about the C(20)−C(21) bond on the NMR time scale. In the $^{13}$C{$^1$H} NMR spectrum, two distinct peaks ($\delta$ 35.4 and 38.1) are observed for the CH vertices as expected. A doublet resonance for the B*C*H(PMe$_3$) nucleus was not seen, presumably due to it being weak and broad. As anticipated, the NMR data for **5b** are similar to those of **5a**.

Interestingly, the crystal structure of **5a** and its NMR data reveal that it is formed as a single diastereoisomer. It would appear that nucleophilic attack of the PMe$_3$ group on **3a** occurs by the phosphine approaching the CH(C$_6$H$_4$Me-4) group at the least sterically crowded side of the molecule.

As mentioned earlier, species with $\eta^5$-7,8-Me$_2$-7,8-C$_2$B$_9$H$_9$ groups often show different reactivity patterns to those having $\eta^5$-7,8-C$_2$B$_9$H$_{11}$ ligands.[6] For this reason, some reactions between **1b** and the reagents [M(≡CC$_6$H$_4$Me-4)(CO)$_2$($\eta^5$-C$_5$H$_5$)] (M = Mo or W) were investigated. In a further extension of the study, the compounds [M(≡CC$_6$H$_4$Me-2)(CO)$_2$($\eta^5$-C$_5$H$_5$)] were also employed as reactants. Although it was anticipated that the latter species would afford compounds in many ways akin to those formed with [M(≡CC$_6$H$_4$Me-4)(CO)$_2$-($\eta^5$-C$_5$H$_5$)], previous studies[23] have shown that changing the aryl group on the alkylidyne carbon from C$_6$H$_4$Me-4 to C$_6$H$_4$Me-2 introduces subtle differences in the relative stability of the final products or even their nature. In the present work, it was hoped that this might help clarify reaction pathways or lead to the discovery of new molecules with unusual structures. In practice, all of the reactions produced a complex mixture of products. Although usually separable by column chromatography, some species, possibly isomers of the major products, were obtained only in small or trace amounts, making full characterization difficult or impossible in all cases.

The species isolated by column chromatography in the reaction between **1b** and [W(≡CC$_6$H$_4$Me-4)(CO)$_2$($\eta^5$-C$_5$H$_5$)] were [WRuO{$\mu$-$\sigma$,$\eta^5$-7,8-Me$_2$-10-CH(C$_6$H$_4$Me-4)-7,8-C$_2$B$_9$H$_8$}(CO)$_2$($\eta^5$-C$_5$H$_5$)] (**4b**), [WRu($\mu$-H){$\mu$-$\eta^5$,$\eta'^5$-7,8-Me$_2$-9-C$_5$H$_4$-10-CH$_2$(C$_6$H$_4$Me-4)-7,8-C$_2$B$_9$H$_7$}(CO)$_5$] (**6a**), and [WRu{$\mu$-$\sigma$,$\eta^5$-2,7-Me$_2$-8-CH$_2$(C$_6$H$_4$Me-4)-9-C(H)O-2,7-C$_2$B$_9$H$_6$}(CO)$_4$($\eta^5$-C$_5$H$_5$)] (**7a**). Compound **6a** was isolated in small amounts and was difficult to separate from **7a**; hence, satisfactory microanalytical data for the former were not obtained.

In the corresponding reaction between **1b** and [W(≡CC$_6$H$_4$Me-2)(CO)$_2$($\eta^5$-C$_5$H$_5$)], the products characterized were two isomers of the oxo−tungsten complex [WRuO{$\mu$-$\sigma$,$\eta^5$-7,8-Me$_2$-*n*-CH(C$_6$H$_4$Me-2)-7,8-C$_2$B$_9$H$_8$}-(CO)$_2$($\eta^5$-C$_5$H$_5$)] ($n$ = 9 (**4c**), 10 (**4d**)) and [RuW{$\mu$-$\sigma$,$\eta^5$-2,7-Me$_2$-8-CH$_2$(C$_6$H$_4$Me-2)-9-C(H)O-2,7-C$_2$B$_9$H$_6$}(CO)$_4$-($\eta^5$-C$_5$H$_5$)] (**7b**). From reactions between **1b** and the molybdenum reagents [Mo(≡CC$_6$H$_4$Me-*n*)(CO)$_2$($\eta^5$-C$_5$H$_5$)] ($n$ = 4 or 2), the products isolated were [MoRu($\mu$-H){$\mu$-$\eta^5$,$\eta'^5$-7,8-Me$_2$-9-C$_5$H$_4$-10-CH$_2$(C$_6$H$_4$Me-4)-7,8-C$_2$B$_9$H$_7$}-(CO)$_5$] (**6b**) and [MoRu($\mu$-H){$\mu$-$\eta^5$,$\eta'^5$-7,8-Me$_2$-9-C$_5$H$_4$-10-CH$_2$(C$_6$H$_4$Me-2)-7,8-C$_2$B$_9$H$_7$}(CO)$_5$] (**6c**), respectively.

Data available for the various complexes are summarized in Tables 1 and 2. Fortunately, characteriza-

(23) (a) Baumann, F-E.; Howard, J. A. K.; Musgrove, R. J.; Sherwood, P.; Stone, F. G. A. *J. Chem. Soc., Dalton Trans.* **1988**, 1879. (b) Howard, J. A. K.; Jeffery, J. C.; Li, S.; Stone, F. G. A. *J. Chem. Soc., Dalton Trans.* **1992**, 627.

**Table 6. Selected Internuclear Distances (Å) and Angles (deg) for [WRuO{$\mu$-$\sigma$,$\eta^5$-7,8-$Me_2$-10-CH($C_6H_4$Me-4)-7,8-$C_2B_9H_8$}$(CO)_2$($\eta^5$-$C_5H_5$)] (4b), with Estimated Standard Deviations in Parentheses**

| | | | | | | | |
|---|---|---|---|---|---|---|---|
| Ru−C(1) | 2.308(8) | Ru−C(2) | 2.33(1) | Ru−B(3) | 2.28 (1) | Ru−B(4) | 2.26 (1) |
| Ru−B(5) | 2.261(9) | Ru−C(5) | 1.86(1) | Ru−C(6) | 1.899 (8) | Ru−W | 2.522 (1) |
| C(1)−C(2) | 1.58(1) | C(1)−B(5) | 1.72(1) | C(1)−B(6) | 1.70(2) | C(1)−B(10) | 1.69(1) |
| C(1)−C(3) | 1.57(1) | C(2)−B(3) | 1.74(1) | C(2)−B(6) | 1.74(1) | C(2)−B(7) | 1.72(2) |
| C(2)−C(4) | 1.53(1) | B(3)−B(4) | 1.82(1) | B(3)−B(7) | 1.81(2) | B(3)−B(8) | 1.77(2) |
| B(4)−B(5) | 1.85 (2) | B(4)−B(8) | 1.80(2) | B(4)−B(9) | 1.80(1) | B(4)−C(10) | 1.71(2) |
| B(4)−W | 2.53(1) | B(5)−B(9) | 1.79(2) | B(5)−B(10) | 1.75(2) | B(6)−B(7) | 1.77(2) |
| B(6)−B(10) | 1.74(2) | B(6)−B(11) | 1.76(2) | B(7)−B(8) | 1.79(2) | B(7)−B(11) | 1.78(1) |
| B(8)−B(9) | 1.80(2) | B(8)−B(11) | 1.82(2) | B(9)−B(10) | 1.77(2) | B(9)−B(11) | 1.76(2) |
| B(10)−B(11) | 1.77(2) | C(5)−O(5) | 1.17(1) | C(6)−O(6) | 1.18(1) | C(10)−H(10A) | 0.96 |
| C(10)−C(11) | 1.46(1) | C(10)−W | 2.064(8) | C(11)−C(12) | 1.41(1) | C(11)−C(16) | 1.37(1) |
| C(12)−C(13) | 1.37(1) | C(13)−C(14) | 1.39(1) | C(14)−C(15) | 1.36(2) | C(14)−C(17) | 1.54 (1) |
| C(15)−C(16) | 1.42(1) | W−O(1) | 1.729(6) | W−C(21) | 2.40(1) | W−C(22) | 2.45 (1) |
| W−C(23) | 2.40(1) | W−C(24) | 2.34(1) | W−C(25) | 2.35(1) | C(21)−C(22) | 1.35 (2) |
| C(21)−C(25) | 1.43(1) | C(22)−C(23) | 1.43(2) | C(23)−C(24) | 1.44(2) | C(24)−C(25) | 1.39 (2) |

| | | | | | | | |
|---|---|---|---|---|---|---|---|
| C(5)−Ru−C(6) | 94.6(4) | C(5)−Ru−W | 98.0(3) | C(6)−Ru−W | 89.2(3) | Ru−B(4)−C(10) | 116.6(6) |
| Ru−B(4)−W | 63.2(2) | C(10)−B(4)−W | 54.1(4) | Ru−C(5)−O(5) | 175.2(8) | Ru−C(6)−O(6) | 175.1(10) |
| B(4)−C(10)−H(10A) | 105.5(5) | B(4)−C(10)−C(11) | 119.0(7) | H(10A)−C(10)−C(11) | 107.0(6) | B(4)−C(10)−W | 83.6(5) |
| H(10A)−C(10)−W | 105.2(3) | C(11)−C(10)−W | 132.6(7) | Ru−W−B(4) | 53.1(2) | Ru−W−C(10) | 94.8(3) |
| B(4)−W−C(10) | 42.3(4) | Ru−W−O(1) | 103.6(2) | B(4)−W−O(1) | 103.7(3) | C(10)−W−O(1) | 102.5(3) |

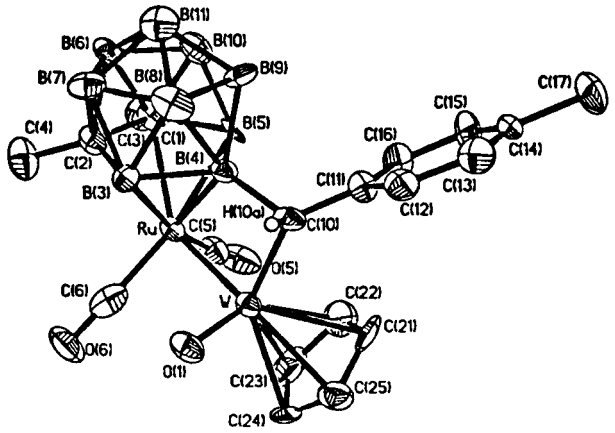


**Figure 4.** Molecular structure of [WRuO{$\mu$-$\sigma$,$\eta^5$-7,8-$Me_2$-10-CH($C_6H_4$Me-4)-7,8-$C_2B_9H_8$}$(CO)_2$($\eta^5$-$C_5H_5$)] (**4b**) showing the crystallographic labeling scheme. Except for H(10a), hydrogen atoms are omitted for clarity. Thermal ellipsoids are shown at 50% probability level.

tion of the complexes was greatly assisted by firm establishment of the molecular structures of compounds **4b**, **6b**, and **7b** by X-ray diffraction. Results of these studies will be reviewed before discussion of the NMR spectra.

The structure of the oxo−tungsten species **4b** is shown in Figure 4, and selected bond distances and angles are listed in Table 6. Like **4a**, complex **4b** was formed in small amounts. Overall, **4b** has a very similar structure to **4a** with one important difference. The exopolyhedral C(H)$C_6H_4$Me-4 substituent on the carborane cage is attached to B(4), the boron atom in the $\beta$ site in the CCB*B*B ring. This is in accord with the above mentioned propensity of $\eta^5$-7,8-$Me_2$-7,8-$C_2B_9H_9$ ligands to direct insertion and other reactions to the B−H bond at the $\beta$ site in the ligating pentagonal ring. Unsurprisingly, several structural parameters for **4b** and **4a** are very similar: Ru−W = 2.514(1) Å (**4a**), 2.522(1) Å (**4b**); W−O(1) = 1.716(5) Å (**4a**), 1.729(6) Å (**4b**); W−C(10) = 2.082(6) Å (**4a**), 2.064(8) Å (**4b**); B(5)−C(10) = 1.62(1) (**4a**), B(4)−C(10) = 1.71(2) Å (**4b**).

The unusual nature of complex **6b** only became recognized after completion of the X-ray diffraction study, the results of which are summarized in Table 7 with the molecule shown in Figure 5. While, as expected, the Ru atom is coordinated by the open CCBBB ring of the carborane cage and the Mo atom is ligated by the $C_5$ ring of the cyclopentadienyl group, the two pentagonal rings are joined (B(3)−C(21) = 1.565(9) Å). The juncture of the two rings occurs at a boron atom which is next to a cage carbon. The carborane framework carries a $CH_2C_6H_4$Me-4 group attached to the $B_\beta$ site in the CCB*B*B ring, and since the cage has Me groups on the carbon vertices, it is likely, following the earlier discussion, that this substituent forms at this site before the linking of the two pentagonal rings. The Mo−Ru distance is very long (3.294(1) Å), and this vector is bridged by a hydrogen atom (Mo−H = 1.85 Å, Ru−H = 1.77 Å, Mo−H−Ru = 131°), the position of which was calculated. The Ru atom carries two CO molecules and the Mo three, all bound in an essentially linear manner.

Although its mode of formation is obscure, the molecular structure of complex **6b** is without precedent. It is interesting to compare **6b** with the dimetallafulvalene complex [MoRu$(CO)_5$($\eta^5$,$\eta'^5$-$C_5H_4$−$C_5H_4$)].[21] The existence of these two molecules emphasizes the relationship between cyclopentadienyl and *nido*-7,8-$Me_2$-7,8-$C_2B_9H_9$ groups as ligands. Fulvalene formally contributes 10 electrons to the MoRu$(CO)_5$ unit in [MoRu$(CO)_5$($\eta^5$,$\eta'^5$-$C_5H_4$−$C_5H_4$)], so overall the complex is saturated with 34 valence electrons. However, the $\mu$-7,8-$Me_2$-9-$C_5H_4$-10-$CH_2$($C_6H_4$Me-4)-7,8-$C_2B_9H_7$ group in **6b** contributes 9 electrons, but this electron deficiency is compensated for by the presence of the $\mu$-H ligand.

The molecule **7b** is shown in Figure 6, and pertinent results from the X-ray diffraction study are summarized in Table 8. The Ru−W bond (2.823(1) Å) is bridged by a very unusual *nido*-2,7-$Me_2$-8-$CH_2$($C_6H_4$Me-2)-9-C(H)O-2,7-$C_2B_9H_6$ cage system. The Ru atom is $\eta^5$-coordinated by an open pentagonal $CB_4$ face (Ru−C(1) = 2.306(7) Å, Ru−B(2) = 2.237(9) Å, Ru−B(3) = 2.224(8) Å, Ru−B(4) = 2.156(8) Å, Ru−B(5) = 2.24(1) Å) with the $CH_2C_6H_4$Me-2 substituent attached to a boron atom (B(2)−C(10) = 1.62(1) Å) adjacent to the CMe group. Unexpectedly, the second CMe group has migrated to a site in the pentagonal ring situated above and parallel

**Table 7. Selected Internuclear Distances (Å) and Angles (deg) for [MoRu($\mu$-H){$\mu$-$\eta^5$,$\eta'^5$-7,8-$Me_2$-9-$C_5H_4$-10-$CH_2$($C_6H_4$Me-4)-7,8-$C_2B_9H_7$}$(CO)_5$] (6b), with Estimated Standard Deviations in Parentheses**

| | | | | | | | |
|---|---|---|---|---|---|---|---|
| Ru−H | 1.77 | Ru−C(1) | 2.221(6) | Ru−C(2) | 2.238(6) | Ru−B(3) | 2.216(7) |
| Ru−B(4) | 2.334(9) | Ru−B(5) | 2.253(9) | Ru−C(13) | 1.884(9) | Ru−C(14) | 1.87(1) |
| Ru−Mo | 3.294(1) | H−Mo | 1.85 | C(1)−C(2) | 1.642(8) | C(1)−B(5) | 1.76(1) |
| C(1)−B(6) | 1.68(1) | C(1)−B(10) | 1.69(1) | C(1)−C(3) | 1.541(9) | C(2)−B(3) | 1.777(9) |
| C(2)−B(6) | 1.69(1) | C(2)−B(7) | 1.71(1) | C(2)−C(4) | 1.521(9) | B(3)−B(4) | 1.81(1) |
| B(3)−B(7) | 1.80(1) | B(3)−B(8) | 1.77(1) | B(3)−C(21) | 1.565(9) | B(4)−B(5) | 1.82(1) |
| B(4)−B(8) | 1.75(1) | B(4)−B(9) | 1.80(1) | B(4)−C(5) | 1.63(1) | B(5)−B(9) | 1.80(1) |
| B(5)−B(10) | 1.78(1) | B(6)−B(7) | 1.76(1) | B(6)−B(10) | 1.69(1) | B(6)−B(11) | 1.75(1) |
| B(7)−B(8) | 1.79(1) | B(7)−B(11) | 1.76(1) | B(8)−B(9) | 1.71(1) | B(8)−B(11) | 1.77(1) |
| B(9)−B(10) | 1.75(1) | B(9)−B(11) | 1.69(1) | B(10)−B(11) | 1.72(1) | C(5)−C(6) | 1.52(1) |
| C(6)−C(7) | 1.38(2) | C(6)−C(11) | 1.42(1) | C(7)−C(8) | 1.38(1) | C(8)−C(9) | 1.38(1) |
| C(9)−C(10) | 1.36(1) | C(9)−C(12) | 1.51(1) | C(10)−C(11) | 1.39(1) | C(13)−O(13) | 1.15(1) |
| C(14)−O(14) | 1.17 (1) | Mo−C(21) | 2.332(6) | Mo−C(22) | 2.333(6) | Mo−C(23) | 2.316(6) |
| Mo−C(24) | 2.305(7) | Mo−C(25) | 2.300(6) | Mo−C(26) | 1.972(8) | Mo−C(27) | 1.972(9) |
| Mo−C(28) | 1.979(7) | C(21)−C(22) | 1.421(8) | C(21)−C(25) | 1.418(8) | C(22)−C(23) | 1.391(9) |
| C(23)−C(24) | 1.419(9) | C(24)−C(25) | 1.417(9) | C(26)−O(26) | 1.17(1) | C(27)−O(27) | 1.17(1) |
| C(28)−O(28) | 1.159(9) | | | | | | |

| | | | | | | | |
|---|---|---|---|---|---|---|---|
| H−Ru−C(13) | 78.9(3) | B(3)−Ru−C(13) | 133.8(3) | B(4)−Ru−C(13) | 91.8(3) | H−Ru−C(14) | 79.5(3) |
| B(3)−Ru−C(14) | 136.4(3) | B(4)−Ru−C(14) | 169.7(4) | C(13)−Ru−C(14) | 88.2(4) | Ru−H−Mo | 131.2(1) |
| Ru−B(3)−B(4) | 70.0(4) | Ru−B(3)−C(21) | 108.3(4) | B(4)−B(3)−C(21) | 124.9(5) | Ru−B(4)−B(3) | 63.1(3) |
| Ru−B(4)−C(5) | 119.1(6) | B(3)−B(4)−C(5) | 125.8(6) | B(4)−C(5)−C(6) | 116.9(6) | Ru−C(13)−O(13) | 176.1(9) |
| Ru−C(14)−O(14) | 176.2(9) | H−Mo−C(21) | 87.2(1) | H−Mo−C(26) | 72.6(2) | C(21)−Mo−C(26) | 120.0(3) |
| H−Mo−C(27) | 129.9(2) | C(21)−Mo−C(27) | 142.8(3) | C(26)−Mo−C(27) | 77.7(4) | H−Mo−C(28) | 70.2(2) |
| C(21)−Mo−C(28) | 119.7(3) | C(26)−Mo−C(28) | 105.6(3) | C(27)−Mo−C(28) | 80.5(3) | B(3)−C(21)−Mo | 116.3(4) |
| Mo−C(26)−O(26) | 179.3(6) | Mo−C(27)−O(27) | 177.4(7) | Mo−C(28)−O(28) | 178.6(7) | | |



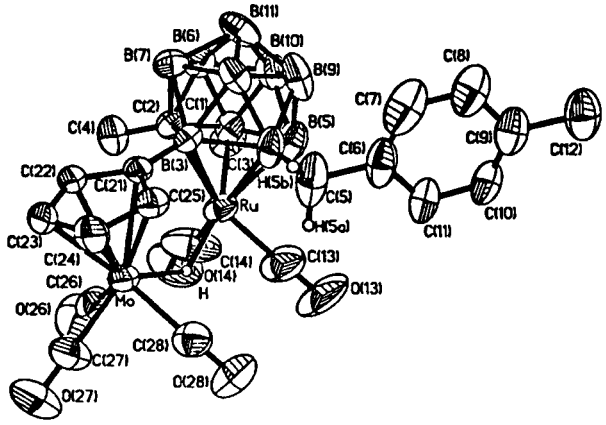


**Figure 5.** Molecular structure of [MoRu($\mu$-H){$\mu$-$\eta^5$,$\eta'^5$-7,8-$Me_2$-9-$C_5H_4$-10-$CH_2$($C_6H_4$Me-4)-7,8-$C_2B_9H_7$}$(CO)_5$] (**6b**) showing the crystallographic labeling scheme. Except for H(5a), H(5b), and the hydrogen atom bridging the Mo−Ru vector, hydrogen atoms are omitted for clarity. Thermal ellipsoids are shown at 50% probability level.

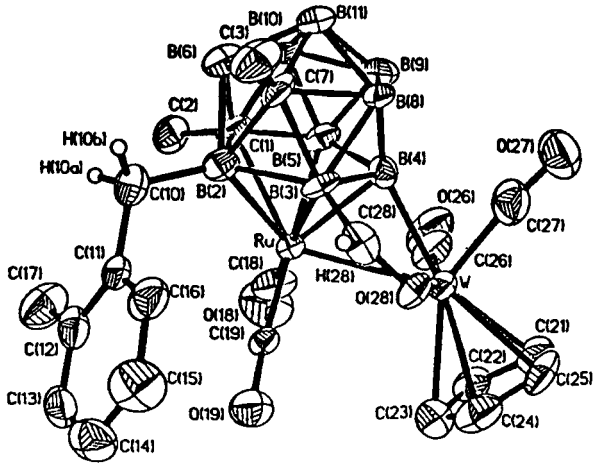


**Figure 6.** Molecular structure of [WRu{$\mu$-$\sigma$,$\eta^5$-2,7-$Me_2$-8-$CH_2$($C_6H_4$Me-2)-9-C(H)O-2,7-$C_2B_9H_6$}$(CO)_4$($\eta^5$-$C_5H_5$)] (**7b**) showing the crystallographic labeling scheme. Except for H(10a), H(10b), and H(28), hydrogen atoms are omitted for clarity. Thermal ellipsoids are shown at 50% probability level.

with that ligating the Ru atom. Such polytopal rearrangements are not uncommon in this area of study,[6b,c] and the process is probably driven in this system by steric requirements. Between B(4) and the tungsten atom there is a $\sigma$ bond (2.26(1) Å). The presence of this link will have influenced the ruthenium to cage atom distances, with Ru−B(4) being the shortest. In addition to B(4), the tungsten is attached to the carborane fragment via a bridging formyl group (W−O(28) = 2.201(5) Å, B(3)−C(28) = 1.54(1) Å, C(28)−O(28) = 1.25(1) Å), which must arise from insertion of a CO molecule into a cage B−H bond. Both metal atoms are coordinated by two CO molecules, and as would be anticipated, the tungsten is ligated by the $C_5H_5$ group.

As a result of the X-ray diffraction work, it was possible to interpret the NMR data obtained for the various complexes. The spectra of **4b**, while showing some very weak signals due to traces of another isomer, are similar in many respects with those of **4a**, due allowance being made for the presence of the cage CMe groups in the former species. In the $^1$H NMR spectrum of **4b**, there are the expected peaks, including a diagnostic resonance for the C(*H*)$C_6H_4$Me-4 nucleus at $\delta$ 7.19. A resonance assignable to the *C*(H)$C_6H_4$Me-4 carbon was not seen in the $^{13}C\{^1H\}$ NMR spectrum, but as mentioned earlier, this is not unusual. The $^{11}B\{^1H\}$ NMR spectrum displayed a resonance at $\delta$ 21.0, which remained as a singlet in a fully coupled $^{11}$B spectrum, as would be expected for the *B*C(H)$C_6H_4$Me-4 nucleus.[6b]

The very weak signals seen in the spectra of **4b** are likely to be due the isomer [WRuO{$\mu$-$\sigma$,$\eta^5$-7,8-$Me_2$-9-CH($C_6H_4$Me-4)-7,8-$C_2B_9H_8$}$(CO)_2$($\eta^5$-$C_5H_5$)] with the bridging CH($C_6H_4$Me-4) fragment attached to the $B_\alpha$ atom in the CC*B*BB ring ligating the ruthenium, as revealed by the X-ray diffraction for **4a**. In this context, it is interesting that the NMR spectra of the oxo complex isolated in small amounts from the reaction between **1b** and [W(≡C$C_6H_4$Me-2)$(CO)_2$($\eta^5$-$C_5H_5$)] showed it to be

**Table 8. Selected Internuclear Distances (Å) and Angles (deg) for [WRu{$\mu$-$\sigma$,$\eta^5$-2,7-Me$_2$-8-CH$_2$(C$_6$H$_4$Me-2)-9-C(H)O-2,7-C$_2$B$_9$H$_6$}(CO)$_4$($\eta^5$-C$_5$H$_5$)] (7b), with Estimated Standard Deviations in Parentheses**

| | | | | | | | |
|---|---|---|---|---|---|---|---|
| Ru−C(1) | 2.306(7) | Ru−B(2) | 2.237(9) | Ru−B(3) | 2.224(8) | Ru−B(4) | 2.156(8) |
| Ru−B(5) | 2.24(1) | Ru−C(18) | 1.856(8) | Ru−C(19) | 1.830(6) | Ru−W | 2.823(1) |
| C(1)−B(2) | 1.72(1) | C(1)−B(5) | 1.72(1) | C(1)−B(6) | 1.72(1) | C(1)−B(10) | 1.73(1) |
| C(1)−C(2) | 1.54(1) | B(2)−B(3) | 1.82(1) | B(2)−B(6) | 1.80(1) | B(2)−C(7) | 1.79(1) |
| B(2)−C(10) | 1.62(1) | B(3)−B(4) | 1.81(1) | B(3)−C(7) | 1.70(1) | B(3)−B(8) | 1.78(1) |
| B(3)−C(28) | 1.54(1) | B(4)−B(5) | 1.83(1) | B(4)−B(8) | 1.79(1) | B(4)−B(9) | 1.78(1) |
| B(4)−W | 2.26(1) | B(5)−B(9) | 1.79(1) | B(5)−B(10) | 1.75(1) | B(6)−C(7) | 1.65(1) |
| B(6)−B(10) | 1.78(2) | B(6)−B(11) | 1.75(1) | C(7)−B(8) | 1.75(1) | C(7)−B(11) | 1.73(1) |
| C(7)−C(3) | 1.52(1) | B(8)−B(9) | 1.71(2) | B(8)−B(11) | 1.75(1) | B(9)−B(10) | 1.80(1) |
| B(9)−B(11) | 1.75(2) | B(10)−B(11) | 1.75(2) | C(10)−C(11) | 1.51(1) | C(11)−C(12) | 1.39(1) |
| C(11)−C(16) | 1.40(1) | C(12)−C(13) | 1.39(1) | C(12)−C(17) | 1.49(1) | C(13)−C(14) | 1.39(1) |
| C(14)−C(15) | 1.36(1) | C(15)−C(16) | 1.39(1) | C(18)−O(18) | 1.18(1) | C(19)−O(19) | 1.209(8) |
| W−C(21) | 2.263(9) | W−C(22) | 2.330(8) | W−C(23) | 2.382(8) | W−C(24) | 2.392(9) |
| W−C(25) | 2.311(8) | W−C(26) | 1.957(9) | W−C(27) | 1.920(8) | W−O(28) | 2.201(5) |
| C(21)−C(22) | 1.40(1) | C(21)−C(25) | 1.42(2) | C(22)−C(23) | 1.37(2) | C(23)−C(24) | 1.41(2) |
| C(24)−C(25) | 1.36(2) | C(26)−O(26) | 1.18(1) | C(27)−O(27) | 1.18(1) | C(28)−H(28) | 0.96 |
| C(28)−O(28) | 1.25(1) | | | | | | |
| C(18)−Ru−C(19) | 87.3(3) | B(4)−Ru−W | 51.8(3) | C(18)−Ru−W | 103.1(3) | C(19)−Ru−W | 88.4(2) |
| Ru−B(3)−C(28) | 113.0(5) | Ru−B(4)−W | 79.5(3) | B(2)−C(10)−C(11) | 117.4(6) | Ru−C(18)−O(18) | 177.4(8) |
| Ru−C(19)−O(19) | 174.6(6) | Ru−W−B(4) | 48.7(2) | Ru−W−C(26) | 75.8(3) | B(4)−W−C(26) | 74.5(3) |
| Ru−W−C(27) | 116.4(3) | B(4)−W−C(27) | 67.8(3) | C(26)−W−C(27) | 86.8(4) | Ru−W−O(28) | 82.6(1) |
| B(4)−W−O(28) | 81.3(3) | C(26)−W−O(28) | 154.6(3) | C(27)−W−O(28) | 91.1(3) | W−C(26)−O(26) | 176.3(7) |
| W−C(27)−O(27) | 172.4(8) | B(3)−C(28)−H(28) | 121.3(4) | B(3)−C(28)−O(28) | 117.7(7) | H(28)−C(28)−O(28) | 121.0(4) |
| W−O(28)−C(28) | 120.3(5) | | | | | | |



mixture of two isomers produced in a ratio of ca. 3:2. Resonances were observed in pairs (Table 2) diagnostic for molecules with structures **4c** and **4d**, respectively, but the isomers were not separable by column chromatography. The weaker set of peaks is attributed to isomer **4d** with the CH(C$_6$H$_4$Me-2) substituent attached to the B$_\beta$ boron in the CCB*B*B ring. This tentative assignment is made on the basis of the values of the chemical shifts observed in the $^1$H and $^{11}$B{$^1$H} NMR spectra of **4d** being similar to those of **4b**, which also has the B$_\beta$ involved in the bridge to the W atom. Thus, in the $^{11}$B{$^1$H} NMR spectra of both molecules, the resonances for the *B*($\mu$-C)W nucleus is observed at $\delta$ 21.0. It is somewhat surprising that the dominant isomer is **4c** rather than **4d**, since the cage carbon atoms carry Me substituents which, from the earlier discussion, would lead to the expectation that **4d** would predominate. However, occasionally with $\eta^5$-7,8-Me$_2$-7,8-C$_2$B$_9$H$_9$ groups we have observed a reaction at the B$_\alpha$−H site in the CC*B*BB ring as the preferred process.[6] Moreover, during separation of the **4c**,**d** mixture from other products by column chromatography it is possible that the initially formed isomer mixture was disturbed. There was no evidence of an equilibrium between the isomers, which would be most unlikely since it would require B−C bond rupture.

Establishment of the structure of **6b** by X-ray diffraction allows interpretation of its NMR data and that of its tungsten analog **6a**. In the $^1$H NMR spectrum of the former, there is a characteristic signal for the $\mu$-H ligand at $\delta$ −17.01[24] and resonances for the nonequivalent cage CMe groups at $\delta$ 2.23 and 2.42. The $\eta^5$-C$_5$H$_4$ group is revealed by the appearance of three multiplets at $\delta$ 4.89, 5.02, and 5.80 of relative intensity 1:1:2. The C$_6$H$_4$Me-4 group displays the normal (AB)$_2$ pattern for the aryl protons ($\delta$ 6.77 and 6.92, with $J$(AB) = 8 Hz) and the customary singlet for the Me-4 group ($\delta$ 1.90). Doublet signals at $\delta$ 1.59 and 1.86 ($J$(HH) = 15 Hz) may be assigned to the diastereotopic protons of the BCH$_2$ group.[25] The $^{13}$C{$^1$H} NMR spectrum shows the expected five signals for the CO ligands ($\delta$ 230.2, 222.7, 221.8 (MoCO) and 196.6, 193.2 (RuCO)) and four resonances for the cage CMe groups ($\delta$ 75.0, 63.8 (*C*Me) and 34.2, 31.0 (C*Me*)). A very broad peak at $\delta$ 30.2 may be assigned to the BCH$_2$ nucleus.[6b] The C$_5$H$_4$ ring displays four ($\delta$ 95.9, 92.6, 92.1, 91.2) rather than the five resonances anticipated, but the peak due to the B*C*(C$_5$H$_4$) nucleus is likely to very broad and is probably lost in the background. The $^{11}$B{$^1$H} NMR spectrum of **6b** shows signals at $\delta$ 10.2 and −0.9 which in a fully coupled $^{11}$B NMR spectrum remain as singlets whereas the other resonances become doublets. These singlets must be due to the BCH$_2$ and BC$_5$H$_4$ groups. The signal at $\delta$ 10.2 is assigned to the *B*CH$_2$ nucleus on the basis of its chemical shift. Resonances in the range $\delta$ 1−12 have been observed in the spectra of many cage compounds containing this group.[6b] A structure with an exopolyhedral metalla-coordinated C$_5$H$_4$ group has not been observed previously, but it seems reasonable to assign the peak at $\delta$ −0.9 to the *B*C$_5$H$_4$ nucleus in view of its singlet character in the $^{11}$B NMR spectrum. The NMR data for **6a** and **6c** are similar to those of **6b**, as expected for molecules having similar structures. The $^{13}$C{$^1$H} NMR spectrum of **6c** (Table 2) reveals, as expected, five peaks for the CO ligands, six resonances for the nonequivalent carbon nuclei of the *C*$_6$H$_4$Me-2 ring, four signals for the cage CMe groups, and a broad resonance assignable to the BCH$_2$ nucleus. There are only three signals attributable to the C$_5$H$_4$ ring, but one peak is of an intensity corresponding to two carbon nuclei, and as with **6b**, it is likely that the resonance due to the B*C*(C$_5$H$_4$) nucleus is so broadened that it is not observed.

It was mentioned earlier that the synthesis of complex **3a** was accompanied by very minor amounts of other species that were difficult to separate by column chromatography. One such species was accumulated from several experiments in a sufficient quantity for mea-

(24) Kaesz, H. D.; Saillant, R. B. *Chem. Rev.* **1972**, *72*, 231.

(25) Brew, S. A.; Stone, F. G. A. *J. Chem. Soc., Dalton Trans.* **1992**, 867. Brew, S. A.; Carr, N.; Jeffery, J. C.; Pilotti, M. U.; Stone, F. G. A. *J. Am. Chem. Soc.* **1992**, *114*, 2203.

surement of its IR and $^1$H NMR spectra. The data (Tables 1 and 2) strongly suggest that it is the complex [WRu($\mu$-H){$\mu$-$\eta^5$,$\eta'^5$-9-$C_5H_4$-10-$CH_2$($C_6H_4$Me-4)-7,8-$C_2B_9H_9$}$(CO)_5$] (**6d**). The band pattern in the CO stretching region of the IR is very similar to that of **6a**−**c**. The $^1$H NMR spectrum displays a diagnostic resonance for the $\mu$-H ligand at $\delta$ −17.55 with $^{183}$W satellite peaks ($J$(WH) = 35 Hz). The presence of the carborane-bound $\eta^5$-$C_5H_4$ group is strongly indicated by the four multiplets observed at $\delta$ 4.78, 5.12, 5.62, and 5.67, each corresponding in intensity to a single proton. The spectrum also displayed two diagnostic doublets ($J$(HH) = 16 Hz) for the two diastereotopic protons of the $BCH_2$ group at $\delta$ 2.25 and 2.33.[25] The complex [MoRu($\mu$-H)-{$\mu$-$\eta^5$,$\eta'^5$-9-$C_5H_4$-10-$CH_2$($C_6H_4$Me-4)-7,8-$C_2B_9H_9$}$(CO)_5$] (**6e**), a molybdenum analog of **6d** was also identified. As expected, its NMR data (Table 2) are very similar to those of **6d**, in accord with the formulation. However, **6e** did not seem to form in the initial synthesis of **3b** but only when the latter was heated in THF. Solutions of **3a** heated in THF produced small amounts of **6d**, but attempts to increase the yield were unsuccessful. The IR and $^1$H NMR spectra of **6e** provide strong evidence that it is structurally similar to **6b**. The IR spectrum shows five CO stretching bands of a similar pattern to the other complexes of type **6** (Table 1). The $^1$H NMR spectrum displays a resonance for the bridging hydride at $\delta$ −16.21 and four multiplets assignable to the $C_5H_4$ group at $\delta$ 4.81, 4.84, 5.63, and 5.70. It seems likely from these observations that the complexes **6a**−**c** form via intermediates similar to the species **3**.

The NMR data (Table 2) for the complexes **7** are in accord with the structure found for **7b** in the solid state. The $^1$H NMR spectrum of the latter shows two peaks for the nonequivalent cage Me groups at $\delta$ 2.06 and 2.49, while the diastereotopic C$H_2$$C_6H_4$Me-2 protons resonate with the expected doublet-of-doublets pattern at $\delta$ 2.75 and 2.85 ($J$(HH) = 17 Hz). A broad peak corresponding to one proton at $\delta$ 10.46 may be assigned to the hydrogen of the BC(H)═O group. As expected, the fully proton-coupled $^{11}$B NMR spectrum had three peaks, which were singlets, in accord with the molecule having three cage boron nuclei attached to substituents other than hydrogen. The signal seen at $\delta$ 57.9 is unambiguously assigned to the B−W group on the basis of its chemical shift.[6b] Hence, the peaks at $\delta$ 1.2 and −10.0 must be due to the $B$$CH_2$ and $B$C(H)O nuclei. The resonance at $\delta$ 1.2 has a chemical shift at the end of the range generally observed for $B$$CH_2$ groups in other molecules,[6b] leaving the signal at $\delta$ −10.0 to be attributed to the $B$C(H)O nucleus. This assignment was confirmed by measuring the $^{11}$B{$^1$H}−$^{11}$B{$^1$H} COSY NMR spectrum, which revealed a connectivity between the nuclei responsible for the peaks at $\delta$ 57.9 and −10.0 but no connectivity between the signals at $\delta$ 57.9 and 1.2. This is in agreement with the results of the X-ray diffraction results (Figure 6) with the $CH_2C_6H_4$Me-2 group attached to B(2), the C(H)O group linked to B(3), and the W atom $\sigma$-bonded to the cage at B(4). The $^{13}$C-{$^1$H} NMR spectrum of **7b** showed the expected four signals for the four nonequivalent CO ligands, and similarly, there were six resonances for the ring carbons of the $C_6H_4$ group (Table 2). The cage CMe groups gave rise to peaks at $\delta$ 63.5 and 62.4 (*C*Me) and at 31.7 and 23.5 (C*Me*). A broad peak occurs at $\delta$ 250.6, which we assign to the B*C*(H)OW nucleus. The metal cluster complex [$MoW_2Pt_2$($\mu$-$CC_6H_4$Me-4)($\mu_3$-$CC_6H_4$Me-4)($\mu_3$-$\sigma$,$\eta^6$-7,9-$Me_2$-12-OC-7,9-$C_2B_{10}H_8$)$(CO)_7$($\eta^5$-$C_5H_5$)$_2$] contains a BOCWPt linkage, and in the $^{13}$C{$^1$H} NMR spectrum, the resonance for the carbon nucleus of the major isomer is at $\delta$ 264.6.[26]

Several hours at room temperature are required for the synthesis of **6a**−**c**. Monitoring by IR and $^{11}$B{$^1$H} NMR spectroscopy revealed transient intermediates with spectral properties similar to those of **2** and **3**. Evidently the nature of the products isolated in the various reactions depends strongly on the presence or absence of Me substituents on the cage carbons of the $C_2B_9$ framework of the reagents **1**.

## Conclusions

The reactions between the ruthenacarborane reagents **1** and the alkylidyne complexes [M(≡$CC_6H_4$Me)$(CO)_2$-($\eta^5$-$C_5H_5$)] (M = Mo or W) were more complicated than first anticipated, since the initially formed dimetal compounds **2**, isolobally related to [Ru$(CO)_2$-(PhC≡CPh)($\eta^5$-7,8-$C_2B_9H_{11}$)],[3c] readily transformed into other products by pathways as yet not fully delineated. It is clear, however, that the complexes **3** play a key role in the overall scheme. Of particular interest is the discovery of complexes of type **6** and **7**, the molecular structures of which have no precedents in organometallic chemistry. In this context, mention was made earlier of the interesting relationship between the $\mu$-$\eta^5$,$\eta'^5$-7,8-$R_2$-9-$C_5H_4$-10-$CH_2$($C_6H_4$Me-*n*)-7,8-$C_2B_9H_7$ (R = H or Me; *n* = 4 or 2) ligands in the complexes **6** and certain dimetal fulvalene complexes.[21]

## Experimental Section

**General Considerations.** Solvents were distilled from appropriate drying agents under nitrogen prior to use. Petroleum ether refers to that fraction of the boiling point 40−60 °C. All reactions were carried out under an atmosphere of dry nitrogen using Schlenk line techniques. Chromatography columns (ca. 15 cm in length and ca. 2 cm in diameter) were packed with silica gel (Aldrich, 70−230 mesh) unless otherwise stated. Celite pads for filtration were ca. 3 cm thick. The reagents [Ru$(CO)_3$($\eta^5$-7,8-$R_2$-7,8-$C_2B_9H_9$)], [$NEt_4$][RuI$(CO)_2$($\eta^5$-7,8-$R_2$-7,8-$C_2B_9H_9$)], and [Ru(THF)$(CO)_2$($\eta^5$-7,8-$R_2$-7,8-$C_2B_9H_9$)] were obtained as described previously.[3] The THF complexes were prepared in THF, but this solvent was subsequently exchanged for $CH_2Cl_2$, in which they are more reactive. The NMR spectra were recorded in $CD_2Cl_2$ at ambient temperatures at the following frequencies: $^1$H at 360.1, $^{13}$C at 90.6, $^{31}$P at 145.8, and $^{11}$B at 115.5 MHz.

**Synthesis of [WRu($\mu$-$CC_6H_4$Me-4)$(CO)_4$($\eta^5$-7,8-$C_2B_9H_{11}$)-($\eta^5$-$C_5H_5$)] (2a).** Complex **1a** was generated *in situ* from [$NEt_4$]-[RuI$(CO)_2$($\eta^5$-7,8-$C_2B_9H_{11}$)] (1.00 g, 1.82 mmol) and $AgBF_4$ (0.35 g, 1.82 mmol) in THF (50 mL). After the mixture was stirred for 10 min, solvent was removed *in vacuo* and the residue dissolved in $CH_2Cl_2$ (50 mL). The solution was filtered through a Celite pad into a solution of [W(≡$CC_6H_4$Me-4)$(CO)_2$($\eta^5$-$C_5H_5$)] (0.74 g, 1.82 mmol) in $CH_2Cl_2$ (25 mL). After the mixture was stirred for 10 min, the volume of solvent was reduced to ca. 5 mL and the mixture chromatographed. Elution with $CH_2Cl_2$−petroleum ether (1:1) initially removed a trace of a red and a green band, followed by a very broad dark red band. After the latter was collected, evaporation of the solvent and washing

(26) Carr, N.; Mullica, D. F.; Sappenfield, E. L.; Stone, F. G. A.; Went, M. J. *Organometallics* **1993**, *12*, 4350.

the residue with petroleum ether (20 mL) gave red microcrystals of [WRu($\mu$-$CC_6H_4$Me-4)$(CO)_4$($\eta^5$-7,8-$C_2B_9H_{11}$)($\eta^5$-$C_5H_5$)] (**2a**, 0.63 g).

**Synthesis of [WRu(CO)$_4${$\sigma$,$\eta^5$-9-CH($C_6H_4$Me-4)-7,8-$C_2B_9H_{10}$}($\eta^5$-$C_5H_5$)] (3a).** Compound **2a** (0.20 g, 0.29 mmol) was dissolved in $CH_2Cl_2$ (25 mL), and the mixture was stirred for 48 h. When the reaction was complete (monitored by IR spectroscopy), the volume of solvent was reduced to ca. 5 mL and chromatographed. Elution with $CH_2Cl_2$−petroleum ether (1:1) gave a broad dark green band. Removal of solvent *in vacuo* and washing the residue with petroleum ether (3 × 5 mL) gave green microcrystals of [WRu$(CO)_4${$\sigma$,$\eta^5$-9-CH($C_6H_4$-Me-4)-7,8-$C_2B_9H_{10}$}($\eta^5$-$C_5H_5$)] (**3a**, 0.09 g).

After the green band containing **3a** had been removed from the chromatography column, elution was continued with $CH_2$-$Cl_2$−petroleum ether (3:1) and a sharp dark red fraction was collected. Removal of solvent *in vacuo* and washing the residue with petroleum ether (2 × 5 mL) yielded purple microcrystals of [WRuO{$\mu$-$\sigma$,$\eta^5$-9-CH($C_6H_4$Me-4)-7,8-$C_2B_9H_{10}$}-$(CO)_2$($\eta^5$-$C_5H_5$)] (**4a**, 0.01 g).

**Synthesis of [MoRu($\mu$-$CC_6H_4$Me-4)$(CO)_4$($\eta^5$-7,8-$C_2B_9H_{11}$)-($\eta^5$-$C_5H_5$)] (2b) and Conversion into [MoRu$(CO)_4${$\sigma$,$\eta^5$-9-CH($C_6H_4$Me-4)-7,8-$C_2B_9H_{10}$}($\eta^5$-$C_5H_5$)] (3b).** Complex **1a** was generated *in situ* from [$NEt_4$][RuI$(CO)_2$($\eta^5$-7,8-$C_2B_9H_{11}$)] (1.00 g, 1.82 mmol) and $AgBF_4$ (0.35 g, 1.82 mmol) in THF (50 mL). After the mixture was stirred for 10 min, solvent was removed *in vacuo* and the residue dissolved in $CH_2Cl_2$ (50 mL). The solution was then filtered through a Celite pad into a solution of [Mo(≡$CC_6H_4$Me-4)$(CO)_2$($\eta^5$-$C_5H_5$)] (0.58 g, 1.82 mmol) in $CH_2Cl_2$ (25 mL). The reaction mixture was immediately worked up by concentrating the volume of solvent *in vacuo* to ca. 5 mL and chromatographing the mixture. Elution with $CH_2Cl_2$−petroleum ether (1:1) removed a broad dark red band, which on removal of solvent *in vacuo* gave a mixture of [MoRu($\mu$-$CC_6H_4$Me-4)$(CO)_4$($\eta^5$-7,8-$C_2B_9H_{11}$)($\eta^5$-$C_5H_5$)] (**2b**) and [MoRu$(CO)_4${$\sigma$,$\eta^5$-9-CH($C_6H_4$Me-4)-7,8-$C_2B_9H_{10}$}($\eta^5$-$C_5H_5$)] (**3b**).

The mixture of **2b** and **3b** isolated as above by column chromatography was dissolved in $CH_2Cl_2$ (25 mL) and stirred for 1 h. The mixture was then concentrated to ca. 5 mL and rechromatographed. Elution with $CH_2Cl_2$−petroleum ether (1:1) removed a dark green band, which on evaporation of solvent *in vacuo* and washing the residue with petroleum ether (2 × 10 mL) gave green microcrystals of **3b** (0.48 g).

**Reactions of the Compounds [MRu$(CO)_4${$\sigma$,$\eta^5$-9-CH($C_6H_4$Me-4)-7,8-$C_2B_9H_{10}$}($\eta^5$-$C_5H_5$)] (M = Mo or W) with $PMe_3$.** (i) Compound **3a** (0.10 g, 0.14 mmol) was dissolved in THF (20 mL), and $PMe_3$ (0.14 mL, 0.14 mmol) was added. The mixture was stirred for 5 min, after which solvent was removed *in vacuo*. The residue was dissolved in $CH_2Cl_2$ (ca. 5 mL) and chromatographed. Elution with $CH_2Cl_2$ removed a broad dark red band, which on evaporation of solvent *in vacuo* and washing the residue with petroleum ether (2 × 10 mL) gave red microcrystals of [WRu$(CO)_4${$\eta^5$-9-CH($PMe_3$)($C_6H_4$Me-4)-7,8-$C_2B_9H_{10}$}($\eta^5$-$C_5H_5$)] (**5a**, 0.09 g).

(ii) Using a similar procedure, **3b** (0.10 g, 0.16 mmol) dissolved in THF (20 mL) with $PMe_3$ (0.16 mL, 0.16 mmol) gave red microcrystals of [MoRu$(CO)_4${$\eta^5$-9-CH($PMe_3$)($C_6H_4$-Me-4)-7,8-$C_2B_9H_{10}$}($\eta^5$-$C_5H_5$)] (**5b**, 0.08 g).

**Reactions of [Ru(THF)$(CO)_2$($\eta^5$-7,8-$Me_2$-7,8-$C_2B_9H_9$)] with [W(≡$CC_6H_4$Me-*n*)$(CO)_2$($\eta^5$-$C_5H_5$)] (*n* = 2 or 4).** (i) The reagent **1b** was generated *in situ* by treating [$NEt_4$][RuI$(CO)_2$-($\eta^5$-7,8-$Me_2$-7,8-$C_2B_9H_9$)] (0.30 g, 0.52 mmol) with $AgBF_4$ (0.10 g, 0.52 mmol) in THF (20 mL). After the mixture was stirred for ca. 10 min, it was chromatographed, eluting with THF. Solvent was removed *in vacuo* from the yellow solution, and the residue obtained was redissolved in $CH_2Cl_2$ (20 mL) and treated with [W(≡$CC_6H_4$Me-4)$(CO)_2$($\eta^5$-$C_5H_5$)] (0.22 g, 0.53 mmol). After the mixture was stirred overnight, solvent was removed *in vacuo*, the dark red residue was extracted with $CH_2Cl_2$−petroleum ether (10 mL, 1:4), and the extract was chromatographed. Elution with $CH_2Cl_2$−petroleum ether (1:4) and evaporation of solvent gave red crystals of [WRu{$\mu$-$\sigma$,$\eta^5$-2,7-$Me_2$-8-$CH_2$($C_6H_4$Me-4)-9-C(H)O-2,7-$C_2B_9H_6$}$(CO)_4$($\eta^5$-$C_5H_5$)] (**7a**, 0.12 g), crystallized from $CH_2Cl_2$−petroleum ether (1:10). Further elution of the column with $CH_2Cl_2$−petroleum ether (2:3) removed an orange-red fraction, which after removal of solvent *in vacuo* gave red crystals of [WRu($\mu$-H)-{$\mu$-$\eta^5$,$\eta'^5$-7,8-$Me_2$-9-$C_5H_4$-10-$CH_2$($C_6H_4$Me-4)-7,8-$C_2B_9$-$H_7$}$(CO)_5$] (**6a**, 0.02 g). Finally, elution with $CH_2Cl_2$ yielded red crystals of [WRuO{$\mu$-$\sigma$,$\eta^5$-7,8-$Me_2$-10-CH($C_6H_4$Me-4)-7,8-$C_2B_9H_8$}$(CO)_2$($\eta^5$-$C_5H_5$)] (**4b**, 0.04 g), after removal of solvent *in vacuo* and crystallization from $CH_2Cl_2$−petroleum ether (1:10).

(ii) Using a similar procedure, **1b** (1.71 mmol) and [W(≡$CC_6H_4$Me-2)$(CO)_2$($\eta^5$-$C_5H_5$)] (0.70 g, 1.71 mmol) gave [WRu{$\mu$-$\sigma$,$\eta^5$-2,7-$Me_2$-8-$CH_2$($C_6H_4$Me-2)-9-C(H)O-2,7-$C_2B_9H_6$}-$(CO)_4$($\eta^5$-$C_5H_5$)] (**7b**, 0.21 g) and [WRuO{$\mu$-$\sigma$,$\eta^5$-7,8-$Me_2$-9-CH($C_6H_4$Me-2)-7,8-$C_2B_9H_8$}$(CO)_2$($\eta^5$-$C_5H_5$)] (**4c**, 0.02 g).

**Reactions of [Ru(THF)$(CO)_2$($\eta^5$-7,8-$Me_2$-7,8-$C_2B_9H_9$)] with [Mo(≡$CC_6H_4$Me-*n*)$(CO)_2$($\eta^5$-$C_5H_5$)] (*n* = 2 or 4).** (i) A $CH_2Cl_2$ (20 mL) solution containing **1b** (0.50 mmol) was prepared as described above and treated with [Mo(≡$CC_6H_4$-Me-4)$(CO)_2$($\eta^5$-$C_5H_5$)] (0.16 g, 0.50 mmol). The reagents were stirred for ca. 5 h, after which solvent was removed *in vacuo* and the dark red residue extracted with $CH_2Cl_2$−petroleum ether (10 mL, 3:7). The extract was chromatographed, and elution with $CH_2Cl_2$−petroleum ether (3:7) gave an orange colored fraction, which after removal of solvent *in vacuo* afforded red crystals of [MoRu($\mu$-H){$\mu$-$\eta^5$,$\eta'^5$-7,8-$Me_2$-9-$C_5H_4$-10-$CH_2$($C_6H_4$Me-4)-7,8-$C_2B_9H_7$}$(CO)_5$] (**6b**, 0.23 g) crystallized from $CH_2Cl_2$−petroleum ether (1:10).

(ii) In a similar procedure, **1b** (0.68 mmol) and [Mo(≡$CC_6H_4$-Me-2)$(CO)_2$($\eta^5$-$C_5H_5$)] (0.22 g, 0.69 mmol) gave [MoRu($\mu$-H){$\mu$-$\eta^5$,$\eta'^5$-7,8-$Me_2$-9-$C_5H_4$-10-$CH_2$($C_6H_4$Me-2)-7,8-$C_2B_9H_7$}$(CO)_5$] (**6c**, 0.10 g).

**Crystal Structure Determinations and Refinements.** Crystals of all species studied (Table 9) were grown by diffusion of a $CH_2Cl_2$ solution into a layer of petroleum ether. The crystal of **5a** was mounted on a glass fiber, and low-temperature data were collected on a Siemens SMART CCD area-detector three-circle diffractometer using Mo Kα X-radiation, $\lambda$ = 0.710 73 Å. For three settings of $\phi$, narrow data "frames" were collected for 0.3° increments in $\omega$. A total of 1321 frames of data were collected, affording rather more than a hemisphere of data. The substantial redundancy in data allows empirical absorption corrections to be applied using multiple measurements of equivalent reflections. Data frames were collected for 20 s per frame. The data frames were integrated using SAINT,[27a] and the structure was solved by conventional direct methods. The structure was refined by full-matrix least-squares on all $F^2$ data, using Siemens SHELX-TL version 5.03,[27b] with anisotropic thermal parameters for all non-hydrogen atoms. The asymmetric unit contains one molecule of the complex and two molecules of $CH_2Cl_2$. One molecule of $CH_2Cl_2$ is disordered with the carbon atom occupying two sites. The agostic B(5)−H(5)⇀W proton was located from a final electron density difference synthesis, and its position was refined. All other hydrogen atoms were included in calculated positions and allowed to ride on the parent boron or carbon atoms with isotropic thermal parameters ($U_{iso}$ = 1.2 × $U_{iso\ equiv}$ of the parent atom, except for Me protons where $U_{iso}$ = 1.5 × $U_{iso\ equiv}$). All calculations were carried out on Silicon Graphics Iris, Indigo, or Indy computers.

The data sets for **3b**, **4a**, **4b**, **6b**, and **7b** were collected on an Enraf-Nonius CAD4-F automated diffractometer operating in the $\omega$−2$\theta$ scan mode, using graphite-monochromated Mo Kα X-radiation. Data were collected at various scan speeds of 0.54−5.17° $m^{-1}$ in $\omega$, with a scan range of 1.15° + 0.34 tan $\theta$. No significant variations were observed in the intensities of the monitored check reflections (<1%). All observed data

(27) (a) *SAINT*. (b) *SHELTXL*, version 5.03. (c) *SHELXTL-PC*, version 4.1, Siemens X-ray Instruments, Madison, WI.

**Table 9. Data for X-ray Crystal Structure Analyses**

| | **3b** | **4a** | **4b** | **5a**·$(CH_2Cl_2)_2$ | **6b** | **7b** |
|---|---|---|---|---|---|---|
| cryst dimens/mm | 0.30 × 0.51 × 0.54 | 0.07 × 0.30 × 0.38 | 0.28 × 0.36 × 0.43 | 0.35 × 0.20 × 0.17 | 0.15 × 0.21 × 0.34 | 0.21 × 0.33 × 0.54 |
| mol form | $C_{19}H_{23}B_9MoO_4Ru$ | $C_{17}H_{23}B_9O_3RuW$ | $C_{19}H_{27}B_9O_3RuW$ | $C_{24}H_{36}B_9Cl_4O_4PRuW$ | $C_{22}H_{27}B_9MoO_5Ru$ | $C_{22}H_{27}B_9O_5RuW$ |
| $M_r$ | 609.7 | 657.6 | 685.6 | 943.5 | 665.7 | 753.6 |
| cryst color, shape | dark, irregular | red plate | red, irregular | red, plate | red, irregular | red, irregular |
| cryst syst | monoclinic | monoclinic | monoclinic | triclinic | monoclinic | monoclinic |
| space group (No.) | $P2_1/c$ (No. 14) | $P2_1/c$ (No. 14) | $P2_1/c$ (No. 14) | $P\bar{1}$ (No. 2) | $P2_1/c$ (No. 14) | $P2_1/c$ (No. 14) |
| $a$/Å | 14.043(2) | 8.702(1) | 8.591(2) | 10.440(3) | 13.501(2) | 13.071(2) |
| $b$/Å | 13.140(1) | 12.770(3) | 20.722(3) | 11.679(4) | 12.874(4) | 10.981(1) |
| $c$/Å | 13.172(3) | 20.212(2) | 14.144(2) | 14.702(4) | 16.122(2) | 18.882(4) |
| $\alpha$/deg | | | | 76.59(3) | | |
| $\beta$/deg | 93.43(1) | 100.35(1) | 105.25(1) | 72.49(3) | 97.86(1) | 96.60(1) |
| $\gamma$/deg | | | | 85.85(4) | | |
| $V$/Å$^3$ | 2426.2(7) | 2209.4(6) | 2429.3(7) | 1663.0(8) | 2775.8(9) | 2692.8(8) |
| $Z$ | 4 | 4 | 4 | 2 | 4 | 4 |
| $D_{calcd}$/g cm$^{-3}$ | 1.669 | 1.977 | 1.875 | 1.884 | 1.593 | 1.860 |
| $\mu$(Mo K$\alpha$)/cm$^{-1}$ | 11.40 | 60.03 | 54.64 | 4.311 | 10.10 | 49.44 |
| $F$(000)/e | 1200 | 1248 | 1312 | 916 | 1320 | 1448 |
| 2$\theta$ range/deg | 3−40 | 3−40 | 3−40 | 5−50 | 3−40 | 3−40 |
| no. of reflns meas | 2526 | 2372 | 2550 | 7948 | 2891 | 2841 |
| no. of unique reflns | 2254 | 2051 | 2257 | 5665 | 2579 | 2507 |
| no. of obsd reflns | 2050 | 1918 | 2120 | | 2262 | 2372 |
| criterion for observed, $n$ [$F_o \geq n\sigma(F_o)$] | $n = 4$ | $n = 4$ | $n = 4$ | | $n = 4$ | $n = 4$ |
| reflection limits | | | | | | |
| $h$ | −13 to +13 | 0 to +8 | 0 to +8 | −12 to +11 | 0 to +12 | 0 to +12 |
| $k$ | 0 to +12 | 0 to +12 | 0 to +19 | −13 to +13 | 0 to +12 | 0 to +10 |
| $l$ | 0 to +12 | −19 to +19 | −13 to +13 | −13 to +17 | −15 to +15 | −18 to +18 |
| final residuals | $R = 0.0202$ | $R = 0.0256$ | $R = 0.0364$ | $wR_2 = 0.097$ | $R = 0.0353$ | $R = 0.0335$ |
| | ($R' = 0.0249$)[a] | ($R' = 0.0291$)[a] | ($R' = 0.0436$)[a] | ($R_1 = 0.035$)[b] | ($R' = 0.0437$)[a] | ($R' = 0.0382$)[a] |
| weighting factors | $g = 0.0001$[a] | $g = 0.0008$[a] | $g = 0.0022$[a] | $a = 0.0511$, $b = 11.183$[b] | $g = 0.0006$[a] | $g = 0.0009$[a] |
| final electron density diff features (max/min)/e Å$^{-3}$ | 0.24/−0.22 | 0.71/−0.94 | 1.58/−1.80 | 0.15/−1.83 | 0.80/−0.66 | 1.63/−0.86 |
| $S$ (goodness-of-fit) | 1.37 | 1.03 | 1.18 | 1.07 | 1.66 | 1.34 |

[a] Refinement was block full-matrix least-squares on $F$ data with a weighting scheme of the form $w^{-1} = [\sigma^2(F_o) + g|F_o|^2]$, where $\sigma^2(F_o)$ is the varience in $F_o$ due to counting statistics: $R = \sum||F_o| - |F_c||/\sum|F_o|$, $R' = \sum w^{1/2}||F_o| - |F_c||/\sum w^{1/2}|F_o|$. [b] Refinement was full-matrix least-squares on all $F^2$ data: $wR_2 = [\sum[w(F_o^2 - F_c^2)^2]/\sum w(F_o^2)^2]^{1/2}$, where $w = [\sigma^2(F_o^2) + (aP)^2 + bP]$ and $P = [\max(F_o^2, 0) + 2F_c^2]/3$. The value in parentheses is given for comparison with refinements based on $F_o$, with a typical threshold of $F \geq 4\sigma(F)$ and $R_1 = \sum||F_o| - |F_c||/\sum|F_o|$, $R' = \sum w^{1/2}||F_o| - |F_c||/\sum w^{1/2}|F_o|$ and $w^{-1} = [\sigma^2(F_o) + g|F_o|^2]$.

were corrected for Lorentz and polarization effects, after which an empirical absorption correction[28] based on nine high-angle $\psi$ scans was carried out. The structures were solved by direct methods, which located most of the non-hydrogen atoms, and successive Fourier difference syntheses were used to locate all remaining non-hydrogen atoms. Refinements were by full-matrix least-squares on $F$ using Siemens SHELXTL-PC version 4.1,[27c] with anisotropic thermal parameters for all non-hydrogen atoms. Methyl, cyclopentadienyl, and phenyl hydrogen atoms were included in calculated positions (C−H = 0.96 Å) for all compounds and constrained to ride on their parent carbon atoms with fixed isotropic thermal parameters ($U_{iso} = 0.08$ Å$^2$). The atoms H(5) and H(10a) in **3b**, H(10a) in the compounds **4**, H(5a) and H(5b) in **6b**, and H(10a), H(10b), and H(28) in **7** were located and similarly treated. The bridging hydrogen atom (H) in compound **6b** was included in a calculated position employing the energy minimization program XHYDEX.[30] Terminal B−H hydrogen atoms for compounds **3b**, **4a**, **4b**, **6b**, and **7b** were included in calculated positions (B−H = 1.10 Å, $U_{iso} = 0.06$ Å$^2$).[29] All refinement calculations were performed on a Siemens PC. Atomic scattering factors were taken from the usual source.[31]

**Acknowledgment.** We thank the Robert A. Welch Foundation for support (Grants AA-1201 and 0668), Dr. Paul Jelliss for helpful discussions, and Dr. James Karban for measurement of a $^{11}B\{^1H\}-^{11}B\{^1H\}$ COSY NMR spectrum.

**Supporting Information Available:** Complete tables of bond lengths and angles, anisotropic thermal parameters, and atom positional and thermal parameters and crystal structures for **3b**, **4a**, **4b**, **5a**, **6b**, and **7b** (58 pages). Ordering information is given on any current masthead page.

OM960928T

(28) *Enraf-Nonius, Vax Structure Determination Package*; Enraf-Nonius: Delft, The Netherlands, 1985.

(29) Sherwood, P. *BHGEN, a program for the calculation of idealized H-Atom positions for a nido-icosahedral carborane cage*; University of Bristol, Bristol, U.K. 1986.

(30) Orpen, A. G. *J. Chem. Soc., Dalton Trans.* **1980**, 2509.

(31) *International Tables for X-ray Crystallography*; Kynoch Press: Birmingham, U.K., 1974; Vol 4.